Optical Properties of Metals: Many-Electron Effects*

L. W. Beeferman and H. Ehrenreich

Division of Engineering and Applied Physics, Harvard University, Cambridge, Massachusetts 02138

(Received 18 August 1969)

The work reported here, which deals with the influence of electron-electron interactions on the optical properties of metals, is motivated by existing discrepancies between the observed interband absorption and that calculated within the random-phase approximation (RPA). These interactions are treated systematically using a self-consistent conserving-approximation scheme. Both vertex and quasiparticle renormalization effects transcending the RPA are considered on an equal footing. Repeated first-order scattering of a quasielectron and a quasihole via the dynamically screened Coulomb interaction is the principal process investigated. The contributions are of two kinds: one associated with a statically screened Coulomb interaction and the other with exchange of virtual plasmons. The latter contribution, although larger than the former, is substantially cancelled, to within about 10% in Al, by quasiparticle dressing effects due to virtual plasmons. Those second-order effects in the dynamically screened interactions, whose inclusion guarantees a conserving approximation, are also negligible. Recent experimental data for Al are reviewed and new theoretical calculations within the RPA presented which appreciably reduce the existing discrepancies. These provide support for the present conclusion that electron-electron interactions do not significantly affect the optical absorption. Previous calculations for Na are discussed and the situation there may well be similar.

I. INTRODUCTION

The quantitative success of band theory in explaining the shape and magnitude of the interband contribution to the dielectric constant has been far more marked in semiconductors than in metals.[1] While recent calculations of semiconductors[2,3] have obtained close agreement with experiment, the corresponding calculations for metals have differed in magnitude by as much as a factor of 3.[4-8] A number of proposals have been put forward for dealing with these discrepancies which have focused either on the effects of the electron-electron interaction resulting from the presence of conduction electrons in metals[8-12] or the fact that the pseudopotential that must be used in calculating optical properties may differ substantially from that used to calculate band structures.[12] In connection with many-electron effects, Hopfield[9] first drew attention to the fact that in the calculation of optical properties, the pseudopotential must be screened by the frequency-dependent dielectric constant appropriate to the incident light. The fact was used in Animalu's[12] subsequent formulation of the optical pseudopotential and its application towards explaining existing discrepancies in the alkali metals. Overhauser[8] addressed himself to the same problem but emphasized instead the role of the exchange interaction which was taken to be unscreened. The results of these efforts may be summarized by noting that the frequency-dependent screening effect is small, provided that the exchange interaction is properly screened. The major corrections within this theoretical framework thus arise from core corrections that are properly included in the optical pseudopotential rather than many-electron effects. These results yield good agreement for potassium.[12] For sodium the predicted absorption is increased by about 50% but still is about a factor of 2 smaller than experimental values.[13] Weiner[14] and Mahan[10,11] have drawn attention to the importance of vertex corrections which describe the interaction of the electron and hole produced by the incident photon. In particular, Weiner showed that the exchange of virtual plasmons between electron and hole can result in a substantial enhancement of the absorption. Mahan[10,11] considered some particular band models for metals and degenerate semiconductors and found that even the statically screened Coulomb interaction, which is responsible for exciton formation in pure semiconductors and insulators, can lead to significant vertex corrections.

The present paper presents a systematic theory that describes the influence of electron interactions on the optical properties of metals, which reduces in the appropriate limits to the results of previous workers, but, in addition, considers effects that have been hitherto neglected. The most important of these is the fact that it is necessary to describe the electron and hole individually as quasiparticles, since in addition to interacting with each other, they are also affected by the other particles in the medium. It will be seen that the quasiparticle ef-

fects are such as essentially to cancel the enhancement produced by the dynamic vertex corrections.[15] The formalism used is that of Martin and Schwinger,[16] and Baym and Kadanoff.[17,18] A conserving approximation is employed which guarantees that the subset of all possible diagrams that is selected is such that the various conservation laws and commutation relations involving particle number, energy, momentum, charge, or current density, as well as the sum rule

$$\int_0^\infty \omega\epsilon_2(\omega)\,d\omega = \tfrac{1}{2}\pi\omega_p^2\,, \qquad (1.1)$$

where ω_p is the plasma frequency, are satisfied. To achieve this it is necessary to consider more complicated vertex corrections involving two Coulomb interactions and multiple electron-hole excitations. These processes are intrinsically of higher order in perturbation theory. The processes to be considered will be characterized physically in terms of a phenomenological calculation in Sec. II, which is intended to serve as an introduction to the more formal treatment that occupies much of the rest of the paper. The principal result of this work is that effects of electron interaction on the optical properties in simple metals appear to be no more than 10 or 20%. This point is elucidated by means of numerical estimates pertaining to the alkali metals and aluminum.

The resolution of the discrepancies between theory and experiment therefore remains an open question. In this connection it should be noted that of the metals (aluminum, copper, potassium, and sodium) investigated in greatest detail the discrepancy in aluminum has appeared to be the most clear cut, since the strong interband transitions are confined to a small region of the frequency spectrum which extends only between about 1 to 3 eV. Thus, it is relatively easy to calculate the entire interband contribution to the dielectric constant separately from that due to the free carriers. Recent calculation of Hughes *et al.*[19] as well as independent work by the present authors[20] have resulted in substantially improved agreement between theory and experiment. In addition to pointing to a possible error in the earlier theoretical results of Ehrenreich, Philipp, and Segall,[4] they also remove one of the strongest arguments for believing that there might be something intrinsically incomplete about a band-theoretic approach to calculation of optical constants in metals as opposed to semiconductors.

We conclude this section with a more explicit outline of the content of the various sections of this paper. The presentation is divided into three main parts. Because of the complexity of the general calculations, the first part, given in Sec. II, is devoted to a phenomenological description of the effects of the electron-electron interaction on the optical absorption. This is based on a model Hamiltonian whose terms describe the principal interactions that need to be considered, and, in particular, virtual-plasmon exchange which is the most important physical mechanism. The contributions of first- and second-order Coulomb and plasmon scattering are estimated. Significant cancellation of the contributions arising from some of these processes is noted.

The second part of the paper comprises Secs. III – VI. These provide a more detailed and rigorous description using the Green's-function formalism. In Sec. III, the relevant notation and formalism is presented. In addition, we discuss the physical basis for the derivation of a formal expression for the optical absorption, including the influence of all interactions. This is written compactly in terms of spectral densities and the vertex function. Section IV begins by defining the conserving approximation which has been selected. An estimate is made of the quasiparticle renormalization factor and a general procedure is outlined which may be used to simplify the integral equation for the vertex function. In Sec. V, this integral equation, including only the first-order effects, is solved approximately and the result is compared with that of other calculations. The cancellation of the dressing effects and vertex corrections, which is responsible for the small contribution of the first-order processes to the optical absorption, is explicitly illustrated. An estimate of the contribution of those higher-order processes in the screened interaction required to produce a conserving approximation is made in Sec. VI. This contribution is seen to be negligible. Since the calculations presented in Secs. IV – VI are extremely lengthy, only the general structure and bare essentials are presented. A detailed exposition may be found in Ref. 20.

In the third part, Sec. VII, the work of Ehrenreich *et al.*[4] is reviewed. New calculations within the random-phase approximation (RPA) using a pseudopotential band structure and pseudowave functions are presented, and, in contrast to the earlier work of Ref. 4, substantial agreement of the magnitude of the interband absorption with experiment is found. Corrections due to the replacement of the pseudowave functions by the true wave functions are considered and shown to be negligible.

II. PHENOMENOLOGICAL DESCRIPTION

Two important considerations underlie the present calculation. First, the electron and the hole are quasiparticles due to their interaction with other particles in the medium. These effects are

described by the self-energy function Σ, labeled by band indices n, a crystal momentum p, and an energy variable, whose real part describes the energy of the particle, and whose imaginary part the lifetime in the state (n, p).

Because of phase-space limitations for scattering near the Fermi surface, it is plausible to speak of independent single-particle-like excitations. These are described by a probability amplitude for being in a particular state which includes a term $Ze^{\mp i\varepsilon_n(p)t - \gamma t}$ [electronlike (−), holelike (+)] where $Z < 1$. $\varepsilon_n(p)$ is the quasiparticle energy and γ the inverse of the lifetime. The remainder of the probability amplitude is weak and broadly spread out in energy.

We expect that it is the sharply defined portion which is dominant in the optical-absorption process. Thus, in all the expressions based on a noninteracting picture, a factor Z must be introduced for each quasiparticle. The net result is to reduce the absorption probability.

The second question relates to the sum rule (1.1), which must be satisfied by any valid approximate calculation of $\mathrm{Im}\epsilon^T$. Since the electron-hole interactions may shift oscillator strength from the Drude intraband to the interband region in metals, if the sum rule is satisfied, an enhancement in the interband range guarantees a reduction in the intraband range. The self-consistent conserving procedure developed by Kadanoff and Baym[17,18] to be used here ensures that an approximation to ϵ^T satisfies (1.1). It requires not only that there be restrictions on the subset of processes for determining the Z's but also that subsets of processes of nominally higher order in perturbation theory be retained.

Because the quasiparticles represent temporally and spatially varying charge disturbances, their interaction must therefore by dynamically screened by a dielectric function dependent on the frequency ω and wave vector q. This dynamically screened interaction may often be treated as being composed of two distinct parts. Classically, the response potential has components in and out of phase with the disturbance, associated with the real and imaginary parts of $\epsilon^{-1}(q, \omega)$. In part, the electron gas responds rigidly and adiabatically to the quasiparticle, perfectly tracking its movement. This part of the effective quasihole-quasielectron interaction is adequately described by the statically screened Coulomb potential and involves $\mathrm{Re}\epsilon^{-1}(q, 0)$.

The second part is out of phase with the disturbance and requires the use of dynamic screening. Most significantly, the quasielectron induces a collective charge disturbance, the plasmon, which propagates through the medium and makes its presence felt at the quasihole and vice versa. This virtual-plasmon exchange is analogous to the virtual-phonon exchange which gives rise to superconductivity. The out-of-phase part is associated with $\mathrm{Im}\,\epsilon^{-1}(q, \omega)$ which, for small q exhibits a sharp peak at $\omega = \omega_P$.

In order to characterize these processes physically, it is useful to introduce the model Hamiltonian

$$
\begin{aligned}
H = &\sum_n \sum_p \varepsilon_n(p)\, c^\dagger_{np}\, c_{np} + \sum_q \varepsilon_P(q)\, a^\dagger_q a_q \\
&+ \sum_{n,n'} \sum_{q,k} g_{nn'}(k, q)\, c^\dagger_{n,k+q} c_{n',k} (a_q + a^\dagger_{-q}) \\
&+ \tfrac{1}{2} \sum_{m,m',n,n'} \sum_{k,k',q} h_{mm'}(k, q)\, h^*_{n'n}(k', q) \\
&\times c^\dagger_{m,k+q} c_{m',k}\, c^\dagger_{n,k'} c_{n',k'+q} \\
&+ \sum_{m,m'} \sum_k (c/2q)^{1/2} (e/m) \\
&\times P_{mm'}(k)\, c^\dagger_{m,k+q} c_{m',k} (b_q + b^\dagger_{-q}) ,
\end{aligned}
\tag{2.1}
$$

and calculate the typical processes described above by perturbation theory. Note that throughout this paper we use units in which $\hbar = 1$. (Vector notation is not explicitly indicated in arguments, subscripts, and summation indices.) The first two terms correspond to the noninteracting electrons of holes and plasmons with energies $\varepsilon_n(p)$ and $\varepsilon_P(q)$, respectively, where all energies are measured from the Fermi level. The vectors are all crystal momenta restricted to the first Brillouin zone and the c's and a's are electron and plasmon field annihilation operators. The third term represents the electron-plasmon coupling and the fourth the statically screened Coulomb interaction. The coupling constants are given by

$$
\begin{aligned}
g_{mm'}(k, q) = &(\delta_{nn'} + (1 - \delta_{nn'}) \{m [\varepsilon_n(k) - \varepsilon_{n'}(k)]\}^{-1} \\
&\times \vec{q} \cdot \vec{P}_{nn'}(k)) \, e |q|^{-1} [\tfrac{1}{2} \Omega^{-1} \varepsilon_P(q)]^{1/2}
\end{aligned}
\tag{2.2a}
$$

and

$$
\begin{aligned}
h_{nn'}(k, q) = &(\delta_{nn'} + (1 - \delta_{nn'}) \{m [\varepsilon_n(k) - \varepsilon_{n'}(k)]\}^{-1} \\
&\times \vec{q} \cdot \vec{P}_{nn'}(k)) \, e |q|^{-1} [\epsilon^{-1}(q, 0)]^{1/2} .
\end{aligned}
\tag{2.2b}
$$

$P_{nn'}(k)$ is the interband momentum matrix element which will be assumed to be constant and real;

$$\varepsilon_n(k) - \varepsilon_{n'}(k) \equiv \varepsilon_{nn'}(k)$$

will also be assumed to be a constant obtained by averaging over the Brillouin zone. Then the g's and h's are independent of k and the two interaction terms are Hermitian. The last two terms of (2.1) correspond, respectively, to the external photon field with energy $\varepsilon [\varepsilon \equiv \varepsilon_{PH}(q)]$ and its interaction with the electrons.

The coupling constants may be interpreted physically by noting first that since the qth component of the electronic charge density is

$$\rho(q) = e \sum_{n,n'} \sum_{k} \langle n,\ k+q \left| e^{-i\vec{q}\cdot\vec{r}} \right| n',\ k \rangle c^{\dagger}_{n,k+q} c_{n,k} \,. \tag{2.3}$$

The term

$$e\langle n,\ k+q \left| e^{-i\vec{q}\cdot\vec{r}} \right| n',\ k \rangle c^{\dagger}_{n,k+q} c_{n,k}$$

describes the charge density produced by the shift of an electron from a Bloch state (n', k) to $(n, k+q)$. For small q,

$$\begin{aligned} &\langle n,\ k+q \left| e^{-i\vec{q}\cdot\vec{r}} \right| n',\ k \rangle \\ &= \int b^{*}_{n}(k+q, r)\, e^{-i\vec{q}\cdot\vec{r}}\, b_{n'}(k, r)\, d^{3}r \\ &= \delta_{nn'} + (1-\delta_{nn'}) \left\{ m \left[\varepsilon_{n}(k) - \varepsilon_{n'}(k) \right]^{-1} \vec{q}\cdot\vec{P}_{nn'}(k) \right\} . \end{aligned} \tag{2.4}$$

By analogy with the electron-phonon problem,[21] the quantity

$$\begin{aligned} &\left[\tfrac{1}{2} \varepsilon_{P}(q)\, \Omega^{-1} \right]^{1/2} (a_{q} + a^{\dagger}_{-q}) \\ &\quad = ne \left[2\varepsilon_{P}(q)\, Nm \right]^{-1/2} (a_{q} + a^{\dagger}_{-q}) \,, \end{aligned} \tag{2.5}$$

where N and n are the number and number density of electrons, respectively, may be written in the form $ne\delta R_{q}$. Here δR_{q} is the qth component of the displacement of the electron gas associated with the plasmon. Thus, the second term in the model Hamiltonian represents the interaction between the electron charge density and the polarization field produced by the plasmon. Similarly, the third term represents the statically screened interaction between the charge densities

$$e \langle m,\ k+q \left| e^{-i\vec{q}\cdot\vec{r}} \right| m',\ k \rangle c^{\dagger}_{m,k+q}\, c_{m',k}$$

and $$e \langle n,\ k' \left| e^{+i\vec{q}\cdot\vec{r}} \right| n,\ k'+q \rangle c^{\dagger}_{n,k'}\, c_{n',k'+q} \,.$$

The photon momentum for typical optical wavelengths may be ignored. A calculation of the absorption due to the creation of an electron-hole pair without Coulomb effects, as shown in Fig. 1(a), yields

$$\begin{aligned} \sigma(\varepsilon) = {} & \tfrac{1}{3} \left(\frac{\varepsilon}{4\pi} \right) \Omega^{-1} \sum_{n,n'} \sum_{p} \left[\left(\frac{e}{m} \right)^{2} \vec{P}^{*}_{nn'}(p) \cdot \vec{P}_{nn'}(p) \right] \\ & \times \left[f(\varepsilon_{n'}(p)) - f(\varepsilon_{n}(p)) \right] \delta(\varepsilon_{n}(p) - \varepsilon_{n'}(p) - \varepsilon) , \end{aligned} \tag{2.6}$$

where $f(x) = (e^{\beta x}+1)^{-1}$ is the the Fermi distribution.

The next more complicated process in which a photon excites an electron and hole which scatter statically within their own bands (n and n', respectively) into an energy-conserving state such that $\varepsilon_{n}(p) - \varepsilon_{n'}(p) = \varepsilon$ is illustrated in Fig. 1(b). The contribution of this to the probability for excitation of a real, final pair is found from second-order perturbation theory to be

$$\begin{aligned} &-\Omega^{-1} \sum_{q} \left[(e/m)\, P^{*}_{nn'}(p-q) \right] h_{n'n'}(p, -q)\, h^{*}_{nn}(p, -q) \\ &\quad \times f(\varepsilon_{n'}(p-q)) \left[\varepsilon - \varepsilon_{n}(p-q) + \varepsilon_{n'}(p-q) \right]^{-1} . \end{aligned} \tag{2.7}$$

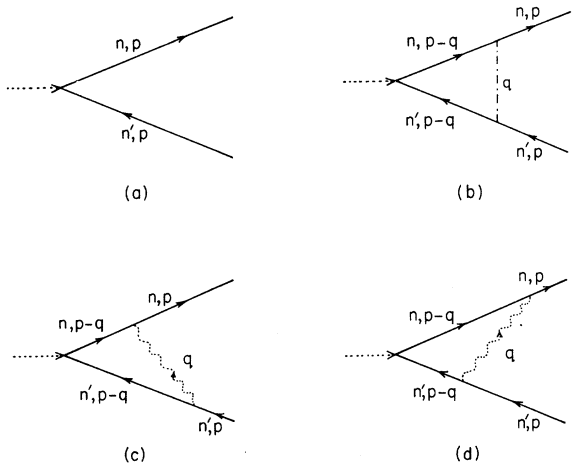

FIG. 1. Typical excitation processes involving creation by an incident photon -----→ of a real quasielectron-quasihole pair; (a) no interaction, corresponding to the RPA result, (b) statically screened scattering -·-·-·- of quasiparticle pair, (c) emission of virtual plasmon (wiggly dotted line) by quasielectron and absorption by the quasihole, and (d) the inverse of process (c).

There are two corresponding virtual-plasmon exchange processes illustrated in Figs. 1(c) and 1(d), respectively, in which the electron or hole emits the virtual plasmon. These make contributions to the probability amplitude for pair excitation in third-order perturbation theory of

$$\begin{aligned} &\Omega^{-1} \sum_{q} \left[(e/m)\, P^{*}_{nn'}(p-q) \right] g_{n'n'}(p, -q)\, g^{*}_{nn}(p, -q) \\ &\quad \times f(\varepsilon_{n'}(p-q)) \left[\varepsilon - \varepsilon_{n}(p-q) + \varepsilon_{n'}(p-q) \right]^{-1} \\ &\quad \times \left[\varepsilon_{P}(q) + \varepsilon_{n'}(p-q) - \varepsilon_{n'}(p) \right]^{-1} \end{aligned} \tag{2.8a}$$

and

$$\begin{aligned} &-\Omega^{-1} \sum_{q} \left[(e/m)\, P^{*}_{nn'}(p-q) \right] g_{n'n'}(p, -q)\, g^{*}_{nn}(p, -q) \\ &\quad \times f(\varepsilon_{n'}(p-q)) \left[\varepsilon - \varepsilon_{n}(p-q) + \varepsilon_{n'}(p-q) \right]^{-1} \\ &\quad \times \left[\varepsilon_{P}(q) + \varepsilon_{n}(p-q) - \varepsilon_{n}(p) \right]^{-1} . \end{aligned} \tag{2.8b}$$

Adding the three contributions from Figs. 1(b)–1(d) yields a correction to the probability amplitude for pair creation of

$$\begin{aligned} &\sum_{q} \left[(e/m)\, P^{*}_{nn'}(p-q) \right] \\ &\times \left\{ h_{n'n'}(p, -q)\, h^{*}_{nn}(p, -q) \left[\varepsilon_{n}(p-q) - \varepsilon_{n'}(p-q) - \varepsilon \right]^{-1} \right. \\ &+ g_{n'n'}(p, q)\, g^{*}_{nn}(p, q) \left[\varepsilon_{P}(q) + \varepsilon_{n'}(p-q) - \varepsilon_{n'}(p) \right]^{-1} \\ &\left. \times \left[\varepsilon_{P}(q) + \varepsilon_{n}(p-q) - \varepsilon_{n}(p) \right]^{-1} \right\} f(\varepsilon_{n'}(p-q)) . \end{aligned} \tag{2.9}$$

Using Eqs. (2.2a) and (2.2b) gives

$$\begin{aligned} &\Omega^{-1} \sum_{q} e^{2} |q|^{-2} \left[(e/m)\, P^{*}_{nn'}(p-q) \right] \\ &\quad \times \left\{ \epsilon^{-1}(q, 0) \left[\varepsilon_{n}(p-q) - \varepsilon_{n'}(p-q) - \varepsilon \right]^{-1} \right. \end{aligned}$$

$$+\tfrac{1}{2}\varepsilon_p(q)[\varepsilon_p(q)+\varepsilon_{n'}(p-q)-\varepsilon_{n'}(p)]^{-1}$$
$$\times[\varepsilon_P(q)+\varepsilon_n(p-q)-\varepsilon_n(p)]^{-1}\}f(\varepsilon_{n'}(p-q))\,. \quad (2.10)$$

Squaring the *total* probability amplitude and taking only the terms linear in the corrections, we obtain exactly the expression for the optical absorption given by Mahan.[10] (He allowed for a single dynamically screened interaction between electron and hole.) His numerical estimates show the second term in the square brackets to make a contribution to the absorption about 10 times that of the first. Mahan's estimate for Na of the second term gives an absorption in the threshold region enhanced about 40% over the RPA value.

Consideration of repeated scattering of the electron and hole should increase the result further: If the RPA probability amplitude is increased by a factor $(1+\alpha)$ to first order in the corrections, then to all orders the correction might be of order $(1-\alpha)^{-1}$. This would give an enhancement factor of nearly 1.6 for sodium. This suggests that much of the discrepancy between theory and experiment for the interband absorption would be removed. Unfortunately though, the argument neglects the fact that it is a quasielectron-quasihole pair, not a bare electron-hole pair which is excited by the photon. Virtual-plasmon exchange also occurs between the electron (or hole) and the medium. If this is taken into account, as described in Sec. III, the subsequent reduction due to the appearance of the Z factors substantially cancels the enhancement just calculated within the errors of our estimates – on the order of 10%. (Exact cancellation can occur in translationally invariant systems for infinitesimal excitations, but not in the present case.) There is what amounts to a destructive interference between the plasmons exchanged with the electron (or hole) and those exchanged with the medium. Although the corresponding detailed calculations for Cu, where plasmons are not as well-defined excitations, have not been carried out, nonetheless we believe that the physical basis for the processes and cancellation just described is also applicable here.

Within the context of this discussion there appears to remain only one possibility for supplying the needed enhancement factor. It has already been noted that a conserving approximation is guaranteed only if higher-order processes are included. These, it turns out, involve two dynamically screened Coulomb interactions. The presence of the two Coulomb factors or other, e.g., phase-space, considerations might make the contribution dominant. Close consideration reveals that this is not the case. For these processes, products of two real parts or products of two imaginary parts of inverse dielectric functions are associated with the "in-phase" response of the system. These, as might have been expected, yield a negligible contribution when compared with the "out-of-phase" response which involves products of one real part and one imaginary part of ϵ^{-1}.

A typical process described by our model Hamiltonian yielding such a term is given in Fig. 2(a). Fourth-order perturbation theory gives a contribution to the probability amplitude for pair excitation of

$$(e/m)\,P^*_{nn'}(p-q)\,g_{n'n'}(p,-q)\,g^*_{nn'}(p,-q)$$
$$\times h^*_{n'n}(p',-q)\,h_{nn}(p',-q)$$
$$\times[\varepsilon_{n'}(p)-\varepsilon_{n'}(p-q)+\varepsilon_n(p'-q)-\varepsilon_{n'}(p')]^{-1}$$
$$\times[\varepsilon_P(q)+\varepsilon_n(p'-q)-\varepsilon_{n'}(p')-\varepsilon]^{-1}\,. \quad (2.11)$$

Another process leading to the same final state, shown in Fig. 2(b), yields

$$-(e/m)\,P^*_{nn'}(p-q)\,g_{n'n'}(p,-q)\,g^*_{nn'}(p,-q)$$
$$\times h^*_{n'n}(p',-q)\,h_{nn}(p',-q)$$
$$\times[\varepsilon_{n'}(p)-\varepsilon_{n'}(p-q)+\varepsilon_n(p'-q)-\varepsilon_{n'}(p')]^{-1}$$
$$\times[\varepsilon_P(q)+\varepsilon_{n'}(p-q)-\varepsilon_n(p)]^{-1}\,. \quad (2.12)$$

Expressions (2.11) and (2.12) do not correspond exactly to the results of the more precise calculations to be discussed in subsequent sections. In

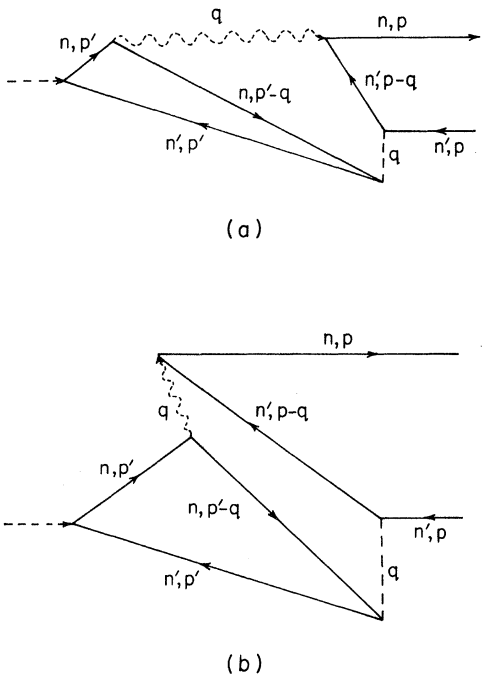

FIG. 2. Second-order processes involving the statically screened interaction and virtual-plasmon exchange corresponding to the Hamiltonian (2.1).

Eqs. (2.11) and (2.12), $\epsilon^{-1}(q, 0)$ should be replaced by $\mathrm{Re}\epsilon^{-1}(q, \omega_P - \omega)$, where $\omega_P(q) \simeq \omega_P$ for small q. The source of the change is the fact that the screening occurs in the presence of the plasmon excitation of frequency ω_P and the charge density induced by the photon frequency ω. This implies the model Hamiltonian is not sufficient to characterize correctly all the processes which we need to consider.

If the necessary corrections to (2.11) and (2.12) are made, the two added, and their contributions added to those of other processes producing the same final state, then they yield a result of only about $\frac{1}{10}$ of that due to the lower-order correction to the absorption. Actually, the complete set of the present type of second-order processes must include also the contributions shown in Figs. 3(a) and 3(b). If these are taken into account, the final result is reduced even further since the contributions of Figs. 2(a) and 2(b) tend to cancel those of Figs. 3(a) and 3(b) and the same is true for the pairs of processes not illustrated here.

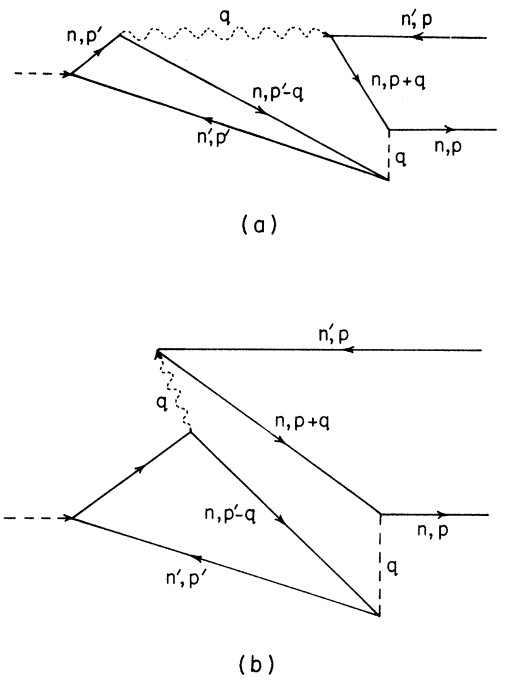

FIG. 3. A pair of second-order processes which tend to cancel the contributions of the processes shown in Fig. 2.

III. DERIVATION OF ABSORPTION COEFFICIENT

This section describes a general procedure for evaluating the optical absorption in solids. The optical properties can be characterized by the macroscopic transverse dielectric function which can be written in terms of the transverse current response function χ^T_{JJ} [22] as

$$\epsilon^T(k, \omega) = 1 + \omega^{-2}(\chi^T_{JJ}(k, \omega) - \omega_P^2), \tag{3.1}$$

for an incident electromagnetic field of wave vector $\vec{k}$ and frequency ω.

A. Formal Preliminaries

The following discussion employs the Green's-function formalism[16,23] which involves the following quantities and relations.

Field operators:

$$\psi_\sigma(r, \tau) = e^{i(H-\mu N)\tau}\,\psi_\sigma(r)\,e^{-i(H-\mu N)\tau}, \tag{3.2a}$$

$$\psi^\dagger_\sigma(r, \tau) = e^{i(H-\mu N)\tau}\,\psi^\dagger_{\sigma(r)}\,e^{-i(H-\mu N)\tau}, \tag{3.2b}$$

where τ is a time variable in the range $(-\infty, +\infty)$ or $(0, -i\beta)$, μ the chemical potential, and N the number operator.

Total Hamiltonian (for imaginary times):

$$H = H_0 + \tfrac{1}{2}\int d^3r_1 d^3r_2 \int_0^{-i\beta} d\tau_2\, \psi^\dagger(r_1, \tau_1)\psi^\dagger(r_2, \tau_2) \times v(r_1, r_2; \tau_1 - \tau_2)\psi(r_2, \tau_2)\psi(r_1, \tau_1)\,. \tag{3.3a}$$

The first term is the one-electron Hamiltonian

$$H_0 = -(2m)^{-1}\int d^3r_1 \psi^\dagger(r_1, \tau_1)\nabla_1^2\psi(r_1, \tau_1) + \int d^3r_1\, u(r_1)\psi^\dagger(r_1, \tau_1)\psi(r_1, \tau_1)\,, \tag{3.3b}$$

containing the *bare* ion potential and the second describes the electron-electron interaction

$$v(r_1, r_2; \tau_1 - \tau_2) = (e^2/4\pi)\,|r_1 - r_2|^{-1}\delta(\tau_1 - \tau_2). \tag{3.4}$$

One- and two-article Green's functions:

$$G(11') = -i\langle T\psi(1)\psi^\dagger(1')\rangle\,, \quad 1 \equiv (r_1, \sigma_1, \tau_1), \tag{3.5}$$

$$G(121'2') = (-i)^2\langle T\psi(1)\psi^\dagger(1')\psi(2)\psi^\dagger(2')\rangle, \tag{3.6}$$

where T is the imaginary time-ordering operator and $\langle\,\rangle$ represents the average over a grand canonical ensemble. In a Bloch representation characterized by basis functions $b_n(p, r)$ and energies $\varepsilon_n(p)$,

$$G_{nm}(p, \omega_\nu) = \int_0^{-i\beta} d(\tau_1 - \tau_{1'})\,[\int d^3r_1 d^3r_{1'}\, b^*_n(p, r_1) \times G(r_1 r_{1'}; \tau_1 - \tau_{1'})\, b_m(p, r_{1'})]e^{-i\omega_\nu(\tau_1 - \tau_{1'})}, \tag{3.7}$$

with fermion frequencies

$$\omega_\nu = i\pi(2\nu + 1)\beta^{-1}, \quad \nu = 0, \pm 1, \pm 2, \ldots\,.$$

Dyson's equation:

$$G^{-1}(11') = G_0^{-1}(11') - \Sigma(11'); \tag{3.8}$$

G_0 and G refer, respectively, to a system described by H_0 and H; Σ is the self-energy.

Spectral representation:

$$G_{nm}(p, \omega_\nu) = \pi^{-1}\int_{-\infty}^{+\infty} A_{nm}(p, x)\,(x - \omega_\nu)^{-1}dx\,; \tag{3.9}$$

$A_{nm}(p, x)$ is the spectral density, a positive-definite Hermitian matrix satisfying

$$\pi^{-1}\int_{-\infty}^{+\infty} A_{mn}(p, x)\,dx = \delta_{nm}\,. \tag{3.10}$$

For the unperturbed system

$$A_{nm}(p, x) = \pi\,\delta_{nm}\,\delta(x - \varepsilon_n(p))\,, \tag{3.11}$$

and $$G_{0;nm}(p, \omega_\nu) = \delta_{nm}\,[\varepsilon_n(p) - \omega_\nu]^{-1}\,. \tag{3.12}$$

Coulomb interaction:

In a plane-wave representation, convenient for later use,

$$v(q, Q) = e^2\,|\vec{q} + \vec{Q}|^{-2}\,. \tag{3.13}$$

$\vec{Q}$ is a reciprocal-lattice vector and q lies in the first Brillouin zone. The fully screened Coulomb interaction (taking into account *all* polarization effects) is $\tilde{V}(11')$ in coordinate space and

$$\begin{aligned}&\tilde{V}(q, Q, Q';\ \omega_\mu)\\ &= \int_0^{-i\beta} d(\tau_2 - \tau_{2'})\,\{\Omega^{-1}\int d^3r_1 d^3r_{1'}\,e^{-i(\vec{q}+\vec{Q})\cdot\vec{r}_1}\\ &\times e^{+i(\vec{q}+\vec{Q}')\cdot\vec{r}_{1'}}\,\tilde{V}(r_1 r_{1'};\ \tau_1 - \tau_{1'})\}\,e^{-i\omega_\mu(\tau_1 - \tau_{1'})}\end{aligned} \tag{3.14}$$

in momentum space; $\omega_\mu = i\pi(2\mu)\beta^{-1}$ are boson frequencies, $\mu = 0, \pm 1, \pm 2, \ldots$.

The quantities (3.14) satisfy Kramers-Kronig relations:

$$\begin{aligned}&\tilde{V}(q, Q, Q';\ z) = \delta_{QQ'}\,v(q, Q)\\ &\quad + \pi^{-1}\int_{-\infty}^{+\infty} \mathrm{Im}\,V(q, Q, Q';\ x)\,(x - z)^{-1}dx,\end{aligned} \tag{3.15}$$

$$\begin{aligned}&\tilde{V}(q, Q, Q';\ z)\,\tilde{V}(k, K, K';\ z + z')\\ &= \delta_{QQ'}\,\delta_{KK'}\,v(q, Q)\,v(k, K)\\ &\quad + \pi^{-1}\int_{-\infty}^{+\infty}[\tilde{V}(q, Q, Q';\ x - z)\\ &\quad \times \mathrm{Im}\,V(k, K, K';\ x)\,(x - z - z')^{-1}\\ &\quad + \mathrm{Im}\,V(q, Q, Q';\ x)\,\tilde{V}(k, K, K';\ x + z)\,(x - z)^{-1}]dx.\end{aligned} \tag{3.16}$$

Here, z and z' are complex frequencies with $\mathrm{Im}(z)$, $\mathrm{Im}(z + z') \neq 0$. For real frequencies,

$$V(q, Q, Q';\ x) = \tilde{V}(q, Q, Q';\ x + i0)\,. \tag{3.17}$$

Response functions:

The current-current correlation function and the current-fluctuation response functions for the α, β Cartesian components are, respectively,

$$\begin{aligned}\chi^{\alpha\beta}_{JJ}(k, K, K';\omega) &= \Omega^{-1}\int d^3r\,d^3r'\int_{-\infty}^{+\infty} d(t - t')\\ &\times e^{-i(\vec{k}+\vec{K})\cdot\vec{r}}\,e^{+i(\vec{k}+\vec{K}')\cdot\vec{r}'}\,e^{i\omega(t-t')}\\ &\times\Theta(t - t')\,\langle[J_\alpha(rt),\ J_\beta(r't')]\rangle\end{aligned} \tag{3.18}$$

and

$$\begin{aligned}&\tilde{\chi}^{\alpha\beta}_{JJ}(k, K, K';\ \omega_\mu) = \Omega^{-1}\int d^3r\,d^3r'\\ &\times\int_0^{-i\beta} d(\tau - \tau')\,e^{-i(\vec{k}+\vec{K})\cdot\vec{r}}\,e^{+i(\vec{k}+\vec{K}')\cdot\vec{r}'}\\ &\times[\langle TJ_\alpha(r\tau)\,J_\beta(r'\tau')\rangle - \langle J_\alpha(r\tau)J_\beta(r'\tau')\rangle]\,.\end{aligned} \tag{3.19}$$

Here

$$J_\alpha(rt) = \left(\frac{e}{2im}\right)\left(\frac{\partial}{\partial r_\alpha}\right) - \left(\frac{\partial}{\partial r_{\alpha'}}\right)\ \psi^\dagger(rt)\,\psi(r't)\,\big|_{r=r'} \tag{3.20}$$

is the current operator, $\theta(x)$ is the Heaviside step function, and ω_μ is a boson frequency. In analogy with Eq. (3.1), the transverse dielectric function is

$$\epsilon^T(k, 0, 0;\ \omega) = 1 + \omega^{-2}(\chi^T_{JJ}(k, 0, 0;\ \omega) - \omega_P^2)\,, \tag{3.21}$$

where χ^T_{JJ} is the transverse component of $\chi^{\alpha\beta}_{JJ}$. Note that

$$\begin{aligned}\mathrm{Im}\,\chi^T_{JJ}(k, 0, 0;\ \omega) &= (2i)^{-1}[\tilde{\chi}^T_{JJ}(k, 0, 0;\ \omega + i0)\\ &- \tilde{\chi}^T_{JJ}(k, 0, 0;\ \omega - i0)]\,.\end{aligned} \tag{3.22}$$

Electron-hole correlation function:

$$L(121'2') \equiv G_2(121'2') - G(11')\,G(22') \tag{3.23}$$

satisfies

$$\begin{aligned}L(121'2') &= -G(12)\,G(21')\\ &+ \int G(1\bar{3})\,G(\bar{4}1')\,\Xi(\bar{3}\bar{5};\ \bar{4}\bar{6})\\ &\times L(\bar{6}2\bar{5}2')\,d\bar{3}\,d\bar{4}\,d\bar{5}\,d\bar{6}\,,\end{aligned} \tag{3.24}$$

where $\Xi(\bar{3}\bar{5};\ \bar{4}\bar{6})$ is the irreducible electron-hole interaction

$$\Xi(\bar{3}\bar{5};\ \bar{4}\bar{6}) = \delta\Sigma(\bar{3}\bar{4})/\delta G(\bar{6}\bar{5}). \tag{3.25}$$

Current- and charge-density vertex functions:

$$\begin{aligned}\Gamma_J(11'2) &= (-e/2im)\,(\nabla_2 - \nabla_{2'})\\ &\times\int G(1\bar{1})\,L(\bar{1}2\bar{1}'2')\,G(\bar{1}'1')\,d\bar{1}\,d\bar{1}'\,\Big|^{\tau_{2'}=\tau_2^+}_{r_{2'}=r_2}\,,\end{aligned} \tag{3.26}$$

$$\Gamma_\rho(1\,1'2) = -\int G(1\bar{1})\,L(\bar{1}2\bar{1}'2)\,G(\bar{1}'1')\,d\bar{1}\,d\bar{1}'\,\Big|^{\tau_{2'}=\tau_2^+}_{r_{2'}=r_2}\,. \tag{3.27}$$

Useful relations involving Γ_J are

$$\begin{aligned}\Gamma_J(1\,1'2) &= (e/2im)\,(\nabla_2 - \nabla_{2'})\,\delta(1\,2')\,\delta(2\,1')\,\Big|^{\tau_{2'}=\tau_2^+}_{r_{2'}=r_2}\\ &- \int \Xi(1\,3\,1'3')\,G(3'\bar{1})\,G(\bar{1}'3)\\ &\times\Gamma_J(\bar{1}\,\bar{1}'2)\,d3\,d3'\,d\bar{1}\,d\bar{1}',\end{aligned} \tag{3.28}$$

$$\begin{aligned}\tilde{\chi}^{\alpha\beta}_{JJ}(1\,2) &= \left(\frac{e}{2im}\right)\left(\frac{\partial}{\partial r_{1f}} - \frac{\partial}{\partial r_{1'\beta}}\right)\int G(1\bar{1})\\ &\times\Gamma^\alpha_J(\bar{1}\,\bar{1}'2)\,G(\bar{1}'1')\,d\bar{1}\,d\bar{1}'\,\Big|^{\tau_{1'}=\tau_1^+}_{r_{1'}=r_1}\,.\end{aligned} \tag{3.29}$$

These are represented diagrammatically in Figs. 4(a) and 4(b).

The transform of Γ_ρ is

$$\begin{aligned}&\Gamma_{\rho,nn'}(p, k;\ Q;\ \omega_\nu,\ \omega_\nu + \omega_\mu,\ \omega_\mu)\\ &= \int_0^{-i\beta} d(\tau_1 - \tau_{1'})\int_0^{-i\beta} d(\tau_1 - \tau_2)\end{aligned}$$

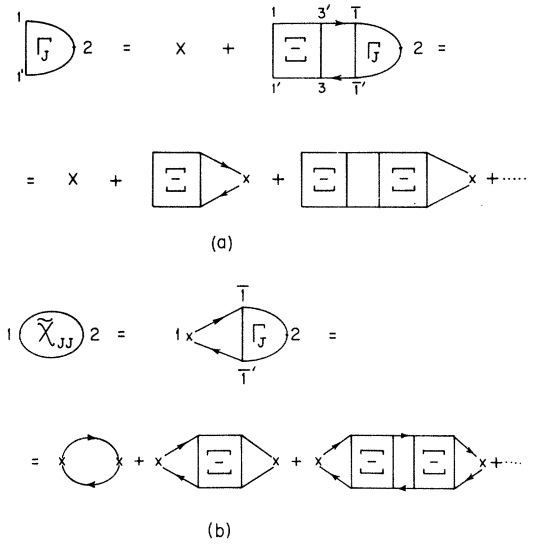

Fig. 4. (a) Diagrammatic representation of the integral equation for the current vertex function Γ_J in terms of the irreducible electron-hole interaction and Green's functions →. The current vertex X corresponds to the first term on the right-hand side of Eq. (3.25). (b) Representation of the equation for the current-fluctuation-response function.

$$\times\Big[\int d^3r_1 d^3r_{1'} d^3r_2\, b_n^*(p+k, r_1)\, e^{i(\vec{k}+\vec{Q})\cdot\vec{r}_1} \times b_{n'}(p, r_{1'})\, \Gamma_\rho(r_1 r_{1'} r_2;\ \tau_1-\tau_{1'},\ \tau_1-\tau_2)\Big] \times e^{i\omega_\nu(\tau_1-\tau_{1'})}\, e^{i\omega_\mu(\tau_1-\tau_2)}\,. \quad (3.30)$$

In the subsequent development only the $Q=0$ component of Γ_J will be required, and we write this as $\Gamma_{J,nn'}(p, k;\ \omega_\nu,\ \omega_\nu+\omega_\mu,\ \omega_\mu)$, suppressing Q. The first term of (3.28) yields the RPA results

$$\Gamma^0_{J,nn'}(p, k) = \int d^3r_2 e^{i\vec{k}\cdot\vec{r}_2}(e/2im)\,(\nabla_2-\nabla_{2'}) \times b_n^*(p+k, r_2)\, b_{n'}(p, r_{2'})\big|_{r_2=r_{2'}} \quad (3.31)$$

and

$$\tilde{\chi}^T_{JJ}(k, 0, 0;\ \omega_\mu) = \tfrac{1}{3}\Omega^{-1}\sum_p \sum_{n,n'} \big|\,\Gamma^0_{J,nn'}(p, k)\,\big|^2 \times\big[f(\varepsilon_{n'}(p)) - f(\varepsilon_n(p+k))\big] \times\big[\varepsilon_n(p+k) - \varepsilon_{n'}(p) - \omega_\mu\big]^{-1}. \quad (3.32)$$

These have the formal structure of the random-phase expression. They were derived using $G \to G_0$, which means the "bare" particle energies and wave functions were employed [cf. Eq. (3.3b)]. Of course, this does not have much physical relation to a solid and is not the way the RPA is usually calculated. Rather the average field produced by the electrons is included in a self-consistent manner by use of Hartree or Hartree-Fock energies and wave functions in Eq. (3.32). Our calculation will encompass a more thorough discussion of quasiparticle corrections and put them on an equal footing with the vertex corrections to be discussed.

B. Broken Diagrams and Formal Expression for Optical Absorption

The objective of this paper is to evaluate $\mathrm{Im}\chi^T_{JJ}$ and hence, $\mathrm{Im}\,\epsilon^T$ including terms that transcend the RPA. In Sec. IV, we note a procedure by which electron-electron interactions may be included in a formal way, yielding an expression which is simpler to evaluate and strikingly similar in *form* to that given in the RPA.

$\mathrm{Im}\,\chi^T_{JJ}$ contains terms involving delta functions which correspond to energy conservation for the processes by which the incident photon creates real excitations in the solid. Examples of such possible excitations are found by imagining that the diagrams of Fig. 4(b) are broken in two by a line so that points 1 and 2 belong to different parts. The particular combination of broken Green's-function lines (or more complicated symbols) thus produced corresponds to a term in $\mathrm{Im}\,\chi^T_{JJ}(k, 0, 0;\ \omega)$ which represents a possible real photon absorption pro-

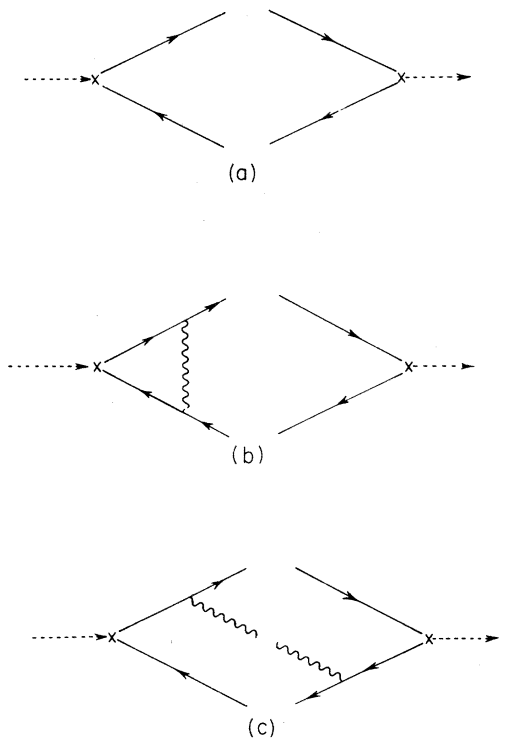

FIG. 5. Broken diagram for the RPA showing excitation (on left) (a) of a real quasiparticle pair, (b) dynamically screened scattering before creation of final pair, and (c) creation of a real plasmon and quasiparticle pair. The diagrams on the right side of the cut correspond to inverse processes.

cess yielding that number of quasielectrons, quasiholes, and other more complicated excitations.

As indicated by Eq. (3.22) and shown in Fig. 5(a), the RPA results simply in the creation of a quasielectron-quasihole pair without vertex corrections. Higher-order processes involve the dynamically screened Coulomb interaction which will be denoted diagrammatically as a solid wiggly line. Any diagram in which a break occurs in such a line may involve the excitation of a plasmon. The four real optical-absorption processes on the left side of the cut correspond to contributions to $\mathrm{Im}\,\chi^T_{JJ}$ involving (a) creation of a non-energy-conserving quasielectron-quasihole pair which scatter via the dynamically screened Coulomb interaction into an energy-conserving final state; (b) creation of an energy-conserving quasielectron-quasihole pair; (c) creation of a non-energy-conserving quasielectron-quasihole pair, and emission of an excitation, such as a plasmon, by the quasihole yielding an energy-conserving final state; (d) the same as (c) with the quasielectron emitting the plasmon. Processes (a) and (d) are illustrated in Figs. 5(b) and 5(c), respectively. Note that the pictures on the right side of the cut in each of the diagrams correspond to the conjugate emission processes.

Our objective is to select from the expression for $\mathrm{Im}\,\chi^T_{JJ}$ those parts which yield a delta function containing the external photon energy and only the energies associated with the quasihole and quasielectron. This is a rather complicated but straightforward procedure which follows the approach of Langer[24] and Ambegaokar[25] and attempts to clarify a number of points and to eliminate some ambiguities.[20] If only virtual scattering processes leading to the creation of a final real quasiparticle pair are considered, one obtains

$$\begin{aligned}\mathrm{Im}\,\chi^T_{JJ}(k,0,0;\omega) = \Omega^{-1}\sum_p \sum_{n,n',m,m'} \pi^{-1} \\ \times \int_{-\infty}^{+\infty} \left([\Phi\Gamma_{J,mm'}(p,k;y,y+\omega,\omega)]^*\right. \\ \times [\Phi\Gamma_{J,nn'}(p,k;y,y+\omega,\omega)] \\ \times A_{m'n}(p+k,y+\omega)A_{n'm}(p,y) \\ \left.\times\{f(y)[1-f(y+\omega)]-f\Phi\Gamma(y+\omega)[1-f(y)]\}\right)dy . \end{aligned} \tag{3.33}$$

The term $\Phi\Gamma_{J,mm'}(p,k;y,y+\omega,\omega)$ is obtained by replacing $\omega_\nu+\omega_\mu$, ω_ν, and ω_μ by $y+\omega$, y, and ω, respectively, and taking principal parts in all the energy denominators containing those terms. This expression is strikingly similar in form to that given in the RPA [Eq. (3.32)] where Γ^0_J is replaced by an effective probability amplitude $\Phi\Gamma_J$ and the bare particle delta functions are replaced by the quasiparticle spectral functions.

IV. EVALUATION OF THE OPTICAL ABSORPTION

This section is concerned first with a discussion of the quasiparticle factors Z which include Hartree and screened exchange corrections. Second, a procedure for simplifying the solution of the integral equation for the vertex function, independent of the approximation, is presented, and its physical significance and relation to other calculations discussed. Finally, the integral equation within the shielded potential approximation is formulated and solved approximately. The cancellation between vertex renormalization and quasiparticle dressing effects is illustrated.

A. Quasiparticle Effects

A prerequisite for evaluation of the optical absorption is selection of an approximation for the irreducible electron-hole interaction Ξ. We want to include in Ξ at least the dynamically screened interaction between the quasielectron and quasihole. It is also desirable to employ the techniques derived by Baym and Kadanoff[17,18] for conserving approximations. Detailed calculations within such a context for optical absorption were first presented by Weiner.[14]

We shall select the shielded potential approximation in which Σ is given by

$$\Sigma(1\,1') = \Sigma_H(1\,1') + \Sigma_s(1\,1') , \tag{4.1}$$

where

$$\Sigma_H(1\,1') = -i\delta(1\,1^+)\int G(2\,2^+)\,v(1'2)\,d2 \tag{4.2}$$

and

$$\Sigma_s(1\,1') = i\tilde{V}_s(1\,1')\,G(1\,1') . \tag{4.3}$$

Equations (4.2) and (4.3) correspond to Hartree and screened exchange corrections, respectively. In the above, $\tilde{V}_s$ satisfies

$$\tilde{V}_s(1\,1') = v(1\,1') - i\int v(1\,\bar{1})\,G(\bar{1}\,\bar{2})\,G(\bar{2}\,\bar{1})\,\tilde{V}_s(\bar{2}\,1')\,d\bar{1}\,d\bar{2} . \tag{4.4}$$

This is the dynamically screened Coulomb interaction within the RPA. Equations (4.2) – (4.4) are illustrated in Figs. 6(a), 6(b), and 7.

Functionally differentiating in accordance with Eq. (3.25) gives

$$\Xi(1\,2\,1'2') = -i\delta(1\,1^+)\,v(1'2)\,\delta(2^+2') \tag{4.5}$$

and

$$\begin{aligned}\Xi_s(1\,2\,1'2') = i\tilde{V}_s(1\,1')\,\delta(1\,2')\,\delta(2\,1^+) + G(2\,2')\,G(1\,1') \\ \times [\tilde{V}_s(1\,2')\,\tilde{V}_s(2\,1') + \tilde{V}_s(1\,2)\,\tilde{V}_s(2'1')]\end{aligned} \tag{4.6}$$

as illustrated in Figs. 6(c) and 6(d).

We treat dressing effects on the same footing as the vertex corrections. For the former, it is necessary to introduce the quasiparticle spectral functions A. Near the Fermi surface, these spectral

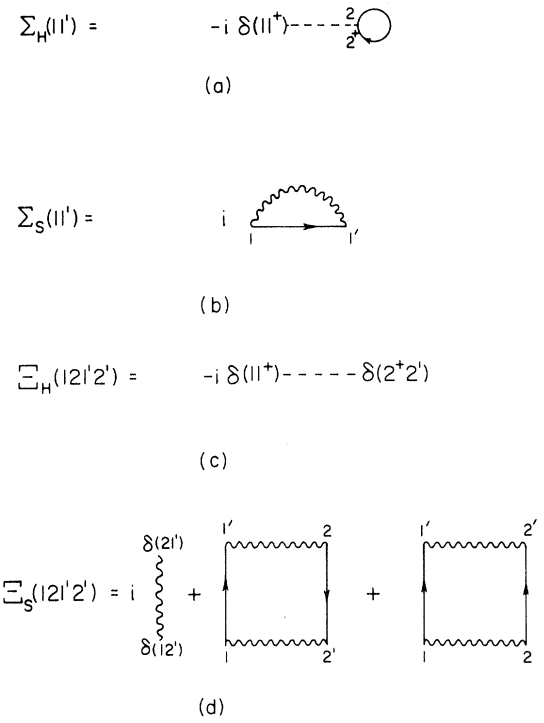

FIG. 6. (a) Hartree and (b) screened exchange contributions to the self-energy Σ within the shielded potential approximation and the corresponding contributions to the irreducible electron-hole interaction, (c) and (d), required by the conserving approximation.

densities may be replaced by the quantities[26]

$$A_{nn'}(p, x) = \delta_{nn'} Z_n(p)\, \delta(x - \varepsilon_n(p)) \ . \tag{4.7}$$

The band indices are now associated with new Bloch basis functions, and quasiparticles of self-energy given by Eq. (4.1). The quasiparticle energies can be regarded as real. The $Z_{n'}(p)$ are the quasiparticle strengths given by

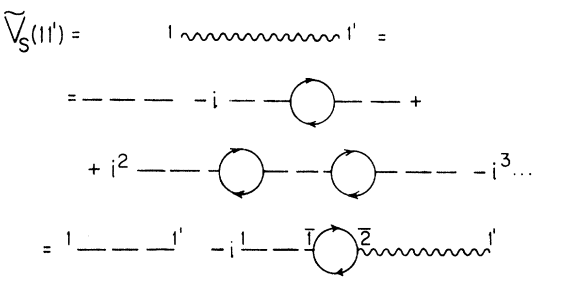

FIG. 7. Integral equation for the dynamically screened interaction in the RPA.

$$Z_{n'}(p) = 1 - \left(\frac{\partial \Sigma_{n'n'}(p, z)}{\partial z} \,\Big|_{z = \varepsilon_{n'}(p) + i0[\varepsilon_{n'}(p)]} \right)^{-1} \tag{4.8}$$

which we shall estimate.

The momentum-frequency transform of Eq. (4.3) is

$$\begin{aligned}\Sigma_{s,nn'}(p, \omega_\beta) &= i\Big[iT \sum_{\omega_\alpha} \Omega^{-1} \sum_{p} \sum_{m,m'} \sum_{Q,Q'} \tilde{\epsilon}^{-1}(p - p', Q, Q'; \omega_\alpha) \\ &\times e^2 |\vec{p} - \vec{p}'|^{-2} (np | e^{i\vec{Q}\cdot\vec{r}_1} | mp') \\ &\times G_{mm'}(p, \omega_\beta - \omega_\alpha)\ (m'p' | e^{-i\vec{Q}\cdot\vec{r}_{1'}} | n'p)\Big] . \end{aligned} \tag{4.9}$$

In the above,

$$\begin{aligned}(np | e^{i\vec{Q}\cdot\vec{r}_1} | mp') &= \int u_n^*(p, r_1)\, e^{i\vec{Q}\cdot\vec{r}_1}\, u_m(p', r_1)\, d^3 r_1 \ , \end{aligned} \tag{4.10}$$

u_n and u_m are the periodic parts of the Bloch functions, and $\tilde{\epsilon}$ is the dielectric function in the RPA. (The Hartree term does not need to be considered, since it is independent of frequency.)

We assume that for the bands and momenta of interest, $G_{m\,m'}$ can be written

$$G_{m\,m'}(p, \omega_\beta) = \delta_{m\,m'} [\varepsilon_m(p) - \omega_\beta]^{-1} \ . \tag{4.11}$$

The frequency sum can be performed to give

$$\begin{aligned}\Sigma_{s,nn'}(p, \omega_\beta) = -\Omega^{-1} \sum_{p'} \sum_{Q,Q'} \sum_{m} & e^2 |\vec{p} - \vec{p}' + \vec{Q}|^{-2} (np | e^{i\vec{Q}\cdot\vec{r}_1} | mp')\, (mp' | e^{-\vec{Q}'\cdot\vec{r}_{1'}} | n'p) \\ &\times \{\tfrac{1}{2}[1 - 2f(\varepsilon_m(p'))]\, \tilde{\epsilon}^{-1}(p - p', Q, Q'; \varepsilon_m(p') - \omega_\beta) + \mathcal{P}\pi^{-1} \\ &\times \int \tfrac{1}{2} \operatorname{sgn}(x) \operatorname{Im} \epsilon^{-1}(p - p', Q, Q'; x) [\varepsilon_m(p') - \omega_\beta - x]^{-1} dx\} \ . \end{aligned} \tag{4.12}$$

Using Eq. (3.15) we can write

$$\begin{aligned}\Sigma_{s,n'n'}(p, z) = -\Omega^{-1} \sum_{p'} \sum_{QQ'} \sum_{m} & e^2 |\vec{p} - \vec{p} + \vec{Q}|^{-2} (n'p | e^{i\vec{Q}\cdot\vec{r}_1} | mp') \\ &\times (mp' | e^{-i\vec{Q}'\cdot\vec{r}_{1'}} | n'p)\ \tfrac{1}{2}[1 - 2f(\varepsilon_m(p'))]\, \delta_{QQ'} + \{\mathcal{P}\pi^{-1} \int_0^\infty \operatorname{Im} \epsilon^{-1}(p - p', Q, Q'; x) \\ &\times [\varepsilon_m(p') - x - z]^{-1} dx\}\ f(\varepsilon_m(p')) \\ &+ \{\mathcal{P}\pi^{-1} \int_{-\infty}^0 \operatorname{Im} \epsilon^{-1}(p - p', Q, Q; x)\, [\varepsilon_m(p') - x - z]^{-1} dx\}\, [1 - f(\varepsilon_m(p'))] \ . \end{aligned} \tag{4.13}$$

Partial differentiation with respect to z yields

$$\frac{\partial \Sigma_{s,n'n'}(p,z)}{\partial z} = -\Omega^{-1}\sum_{p'}\sum_{Q,Q'}\sum_{m} e^2|\vec{p}-\vec{p}'+\vec{Q}|^{-2}(n'p|e^{i\vec{Q}\cdot\vec{r}_1}|mp')(mp'|e^{-i\vec{Q}\cdot\vec{r}_{1'}}|n'p)$$
$$\times\{\mathcal{P}\pi^{-1}\int_0^\infty \mathrm{Im}\,\epsilon^{-1}(p-p',Q,Q';x)\,[\varepsilon_m(p')-x-z]^{-2}\,dx\}f(\varepsilon_m(p'))$$
$$+\{\mathcal{P}\pi^{-1}\int_{-\infty}^0 \mathrm{Im}\,\epsilon^{-1}(p-p',Q,Q';x)\,[\varepsilon_m(p')-x-z]^{-2}\,dx\}\,[1-f(\varepsilon_m(p'))]\ . \qquad (4.14)$$

Now, we let $z \to \varepsilon_{n'}(p) - i0$ (for a quasihole); in this case, since the energy denominators in Eqs. (4.14) will never vanish in the range of p we are considering, we can neglect the $i0$. Observe that if $p = p_F$, both integrals in Eq. (4.14) are negative definite.

As before, the product of matrix elements and the Coulomb factor gives the largest contribution for $Q = 0$. Using, for small $|\vec{p}-\vec{p}'|$,

$$\mathrm{Im}\,\epsilon^{-1}(p-p',0,0;x) = -\tfrac{1}{2}\pi^{-1}\varepsilon_P[\delta(x-\varepsilon_P)-\delta(x+\varepsilon_P)], \qquad (4.15)$$

it is found that

$$\left.\frac{\partial \Sigma_{s,n'n'}(p,z)}{\partial z}\right|_{z\to\varepsilon_{n'}(p)-i0} = -\tfrac{1}{2}\varepsilon_P|M|^2\Omega^{-1}\sum_{p',\,|p-p'|<q_c} e^2|\vec{p}-\vec{p}'|^{-2}$$
$$\times f(\varepsilon_{n'}(p'))\,[\varepsilon_{n'}(p')-\varepsilon_{n'}(p)-\varepsilon_P]^{-2}. \qquad (4.16)$$

Corrections from terms for which $Q \neq 0$ increase the magnitude of the result slightly. $|M|^2$ is an average of $|(n'p|n'p')|^2$ over the allowed values of p'.

We define

$$\alpha_{n'}(p) = \left.\frac{-\partial \Sigma_{n'n'}(p,z)}{\partial z}\right|_{z\to\varepsilon_{n'}(p)-i0}, \qquad (4.17)$$

so that $Z_{n'}(p) = 1 + \alpha_{n'}(p)$. (4.18)

Using similar procedures, we can construct

$$Z_n(p+k) = 1 + \alpha_n(p+k) \qquad (4.19)$$

for a quasielectron.

B. Vertex Corrections: Rearrangement of Hartree Terms

Some simplification of the solution of the integral equation for Γ_J eliminates the necessity for including the Ξ_H term. Suppose that *any* approximation for Ξ is written as $\Xi_H + \Xi_E$. (Ξ_E in our approximation will be taken to be Ξ_S.)

We define

$$\tilde{V}_E(1\,2) = v(1\,2) - \int v(1\,3)\,\tilde{\Pi}^E_{\rho\rho}(3\,4)\,\tilde{V}_E(4\,2)\,d3\,d4\ , \qquad (4.20)$$

where

$$\tilde{\Pi}^E_{\rho\rho}(3\,4) = i\int G(3\,1)\,G(1'3)\,\Gamma^E(1\,1'4)\,d4\,d4' \qquad (4.21)$$

and

$$\Gamma^E(1\,1'4) = \delta(1\,4)\,\delta(4\,1') - i\int \Xi_E(1\,\bar{3}\,1'\bar{3}')$$
$$\times G(\bar{3}'4)\,G(\bar{4}'3)\,\Gamma^E(\bar{4}\,\bar{4}'4)\,d\bar{3}\,d\bar{3}'\,d\bar{4}\,d\bar{4}'\ . \qquad (4.22)$$

$\Pi^E_{\rho\rho}$ can be seen to be the irreducible polarization operator and hence, if $\Xi_H + \Xi_E$ is the complete Ξ, then $\tilde{V}_E$ is the fully screened Coulomb interaction $\tilde{V}$. Otherwise, $\tilde{V}_E$ is some approximation to $\tilde{V}$. By considering the first term of Eq. (4.22), it is seen that $\tilde{V}_E$ always contains at least the polarization bubbles which characterize the RPA. If we solve Eq. (3.24) with Ξ replaced by Ξ_E and by analogy with Eqs. (3.26) and (3.27), define $\Gamma^E_J(1\,1'2)$ and $\Gamma^E_\rho(1\,1'2)$ we find

$$\Gamma_J(1\,1'2) = \Gamma^E_J(1\,1'2) - i\int \Gamma^E_\rho(1\,1'5)\,\tilde{V}_E(5\,\bar{3})$$
$$\times G(\bar{3}\,\bar{4})\,G(\bar{4}'\bar{3})\,\Gamma^E_J(\bar{4}\,\bar{4}'2)\,d5\,d\bar{4}\,d\bar{4}'\,d\bar{3}\ . \qquad (4.23)$$

Introduction of

$$\tilde{\Pi}^E_{\rho J}(\bar{3}\,2) = \int G(\bar{3}\,\bar{4})\,G(\bar{4}'\bar{3})\,\Gamma^E_J(\bar{4}\,\bar{4}'2)\,d\bar{4}\,d\bar{4}' \qquad (4.24)$$

implies that

$$\Gamma_J(1\,1'2) = \Gamma^E_J(1\,1'2) + \int \Gamma^E_\rho(1\,1'2)\,\tilde{V}_E(\bar{2}\,\bar{2}')$$
$$\times\tilde{\Pi}^E_{\rho J}(\bar{2}'2)\,d\bar{2}\,d\bar{2}', \qquad (4.25)$$

which is shown in Fig. 8.

By analogy with Eqs. (3.30), (3.18), and (3.14), we define

$\Gamma^E_{J,nn'}(p,k;\omega_\nu,\omega_\nu+\omega_\mu,\omega_\mu)$,

$\Gamma_{J,nn'}(p,k;\omega_\nu,\omega_\nu+\omega_\mu,\omega_\mu)$,

$\tilde{\Pi}^E_{\rho J}(k,Q,Q';\omega_\mu)$, and $\tilde{V}_E(q,Q,Q';\omega_\mu)$.

Then, Eq. (4.25) becomes

$$\Gamma_{J,nn'}(p,k;\omega_\nu,\omega_\nu+\omega_\mu,\omega_\mu)$$
$$= \Gamma^E_{J,nn'}(p,k;\omega_\nu,\omega_\nu+\omega_\mu,\omega_\mu)$$
$$- i\sum_{Q,Q'}\Gamma^E_{\rho,nn'}(p,k;Q;\omega_\nu,\omega_\nu+\omega_\mu,\omega_\mu)$$

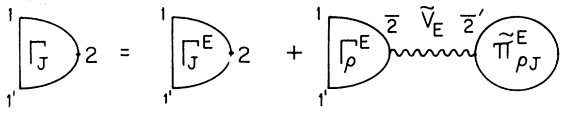

FIG. 8. The equation for Γ_J showing the two contributions, Γ_J^E corresponding to direct coupling with the currents in the system and $\Gamma_\rho^E \tilde{V}_E \Pi_{\rho J}^E$ corresponding to indirect coupling to induced charge densities.

$$\times \tilde{V}_E(k, Q, Q';\ \omega_\mu)\, \tilde{\Pi}^E_{\rho J}(k, Q', 0; \omega_\mu). \qquad (4.26)$$

Previously, it was remarked that when appropriately analytically continued, Γ_J may be treated as an effective probability amplitude for pair creation. It is now seen that this probability amplitude is composed of two distinct parts. The first corresponds to the first term of Eq. (4.25) and can be associated with an effective probability amplitude for pair excitation due to direct coupling to the currents induced by the photon field. The second describes the fact that the system, in responding to the probe, induces a charge density characterized by $\Pi^E_{\rho J}$. This charge density can exert its influence elsewhere in the system via a screened Coulomb interaction $\tilde{V}_E$. Given this charge-density disturbance, there is an effective probability amplitude for pair excitations characterized by Γ^E_ρ.

In terms of a dielectric function

$$\epsilon_E^{-1}(1\,3) = \delta(1\,3) + \int v(1\,4)\, \tilde{\chi}^E_{\rho\rho}(4\,3)\, d4\,, \qquad (4.27)$$

we may write

$$\tilde{V}_E(1\,2) = \int \tilde{\epsilon}_E^{-1}(1\,3)\, v(3\,2)\, d3. \qquad (4.28)$$

For a model in which the effective screened lattice potential U^{sc}_Q is weak, it can be shown that

$$\Gamma_{J,n\,n'}(p, k; \omega_\nu, \omega_\nu + \omega_\mu, \omega_\mu) \simeq \Gamma^E_{J,n\,n'}(p, k; \omega_\nu, \omega_\nu + \omega_\mu, \omega_\mu) \times \tilde{\epsilon}_E^{-1}(k, Q_{n\,n'}, Q_{n\,n'}; \omega_\mu), \qquad (4.29)$$

where $Q_{n\,n'} = Q_n - Q_{n'}$ and Q_n and $Q_{n'}$ are the reciprocal-lattice vectors associated with bands n and n' in an extended-zone scheme.[27]

This result is similar to those obtained by Hopfield,[9] Overhauser,[8] and Animalu.[12] In the work of Hopfield, it is assumed that the self-consistently screened one-electron lattice potential is weak. For $T = 0$, he describes the response to a uniform external electric field, treating the electron-electron interactions exactly and the lattice potential to second order. With these same assumptions, Eq. (3.33) yields the same results for quasiparticle pair creation as Hopfield's Eq. (6).[20] In Overhauser's calculation the response to the photon field is considered, including explicitly the influence of the self-consistently determined Hartree and exchange potentials the latter of which are taken to be unscreened. But as Overhauser and Animalu point out, if screened exchange is employed, the net influence of the exchange correction is negligible. Then the factor ϵ_E^{-1} is relatively unimportant: It tends to reduce Γ_J^E by about 10%. Thus, without the other vertex corrections which are to be discussed, the calculated absorption might be less than that in the RPA.

V. FIRST-ORDER CORRECTIONS

In this section, the contribution of first-order processes will be estimated and the cancellation between vertex and quasiparticle corrections exhibited. To accomplish this, the simplified integral equation for Γ_J^E is solved excluding higher-order effects.

Assuming that $\Xi_E = \Xi_S$ and using Eq. (4.6), the integral equation for Γ_J^E becomes

$$\Gamma^E_J(1\,1'2) = e(2im)^{-1}(\nabla_2 - \nabla_{2'})\,\delta(1\,2')\,\delta(2\,1')\big|_{2'=2^+} + \int \{i\,\tilde{V}_S(1\,1')\,\delta(1\,3')\,\delta(3\,1') + G(3\,3')\,G(1\,1')\,[\tilde{V}_S(1\,3')\,\tilde{V}_S(3\,1') + \tilde{V}_S(1\,3)\,\tilde{V}_S(3'1')]\}\,G(3'4)\,G(4'3)\,\Gamma^E_J(4\,4'2)\,d4\,d4'\,d3\,d3'. \qquad (5.1)$$

Introducing the momentum-frequency transform of Γ_J^E and performing the space and time integrations gives

$$\Gamma^E_{J,nn'}(p,k;\omega_\nu,\omega_\nu+\omega_\mu,\omega_\mu) = \Gamma^0_{J,nn'}(p,k) + iT\sum_{\omega_\gamma}\sum_{Q,Q'}\Omega^{-1}\sum_{p'}\sum_{m,m',l,l'}\{e^2\big|\vec{p}-\vec{p}\,'+\vec{Q}\big|^2 \times \tilde{\epsilon}^{-1}(p-p',Q,Q';\omega_\nu-\omega_\gamma)(np+k\,|\,e^{i\vec{Q}\cdot\vec{r}_1}|\,lp'+k)\,(m'p'\,|\,e^{-i\vec{Q}'\cdot\vec{r}_{1'}}|\,np)$$

$$+ iT\sum_{\omega_\alpha}\sum_{\bar{Q},\bar{Q}'}\Omega^{-1}\sum_{q}\sum_{\bar{m},\bar{m}',\bar{l},\bar{l}'} e^2\big|\vec{q}+\vec{\bar{Q}}\big|^{-2}\tilde{\epsilon}^{-1}(q,Q,Q';\omega_\alpha)e^2\big|\vec{q}+\vec{k}+\vec{\bar{Q}}\big|^{-2} \times \tilde{\epsilon}^{-1}(q+k,\bar{Q},\bar{Q}';\omega_\alpha)G_{\bar{m}\bar{m}'}(p-q;\omega_\nu-\omega_\alpha)(np+k\,|\,e^{i\vec{\bar{Q}}\cdot\vec{r}_1}|\,\bar{m}p-q)(\bar{m}'p'-q\,|\,e^{-i\vec{\bar{Q}}'\cdot\vec{r}_{1'}}|\,n'p)$$

$$\times[(m'p'|e^{-i\vec{\bar{Q}}\cdot\vec{r}_3}|\bar{l}p'-q)G_{\bar{l}\bar{l}'}(p'-q;\omega_\gamma-\omega_\alpha)(\bar{l}'p'-q|e^{-i\bar{Q}'\cdot\vec{r}_{3'}}|lp')$$

$$+(m'p'|e^{-\vec{\bar{Q}}'\cdot\vec{r}_3}|\bar{l}p'+q+k)G_{\bar{l}\bar{l}'}(p'+q+k;\omega_\alpha+\omega_\gamma+\omega_\mu)(\bar{l}'p'+q+k|e^{i\vec{Q}\cdot\vec{r}_{3'}}|lp'+k)]\}$$

$$\times G_{ll'}(p+k,\omega_\gamma+\omega_\mu)G_{mm'}(p',\omega_\gamma)\Gamma^E_{J,l'm}(p',k;\omega_\gamma,\omega_\gamma+\omega_\mu,\omega_\mu)\ . \tag{5.2}$$

Effects arising when sums of momenta such as $\vec{p}+\vec{q}+\vec{k}$ do not lie in the first Brillouin zone will be ignored because they are small.

The integral equation which Weiner[14] attempted to solve is obtained if the higher-order terms in square brackets are ignored. He chose an analytic-continuation procedure for Γ_J somewhat similar to the one we have discussed and the result was substituted into an expression analogous to Eq. (5.2). However, the spectral functions associated with the true propagators were replaced by delta functions since he used non-interacting Green's functions.

We now temporarily ignore the last two terms in square brackets on the right side of Eq. (5.2) and replace each Green's function with the approximation given by Eq. (4.11). Proceeding as Weiner, we assume that Γ_J is a slowly varying function of ω_γ so that it may be removed from the sum and evaluated at $\omega_\gamma=\omega_\nu$. Performing the frequency sums, letting $T\to 0$ and selecting the appropriate analytic continuation gives

$$\mathcal{P}\Gamma^E_{J,nn'}(p,k;\varepsilon_{n'}(p),\varepsilon_n(p+k),\varepsilon)=\Gamma^0_{J,nn'}(p,k)$$

$$+\Omega^{-1}\sum_{P'}\sum_{Q,Q'}\sum_{l,m}e^2|\vec{p}-\vec{p}'+\vec{Q}|^{-2}(n,p+k|e^{i\vec{Q}\cdot\vec{r}_1}|l,p'+k)(mp'|e^{-i\vec{Q}'\cdot\vec{r}_{1'}}|n'p)$$

$$\times[\varepsilon_l(p'+k)-\varepsilon_m(p')-\varepsilon]^{-1}\left(\tfrac{1}{2}[1-2f(\varepsilon_m(p'))]\,\mathrm{Re}\,\epsilon^{-1}(p-p',Q,Q';\varepsilon_m(p')-\varepsilon_{n'}(p))\right.$$

$$\left.-\tfrac{1}{2}[1-2f(\varepsilon_l(p'+k))]\,\mathrm{Re}\,\epsilon^{-1}(p-p',Q,Q';\varepsilon_m(p'+k)-\varepsilon_n(p+k))\right)$$

$$+\mathcal{P}\pi^{-1}\int_{-\infty}^{+\infty}\tfrac{1}{2}\,\mathrm{sgn}(x)\,\mathrm{Im}\,\epsilon^{-1}(p-p',Q,Q';x)\{[\varepsilon_m(p')-\varepsilon_{n'}(p)-x]^{-1}$$

$$-[\varepsilon_l(p'+k)-\varepsilon_n(p+k)-x]^{-1}\}dx\Big)\mathcal{P}\Gamma^E_{J,lm}(p',k;\varepsilon_{n'}(p),\varepsilon_n(p+k),\varepsilon), \tag{5.3}$$

where $\mathcal{P}$ means a principal-parts integration about the point $x=0$ and any point at which an energy denominator vanishes. Using Eq. (3.15) and rearranging terms yields

$$\mathcal{P}\Gamma^E_{J,nn'}(p,k;\varepsilon_{n'}(p),\varepsilon_n(p+k),\varepsilon)\simeq\Gamma^0_{J,nn'}(p,k)+\Omega^{-1}\sum_p\sum_{Q,Q'}\sum_{l,m}e^2|\vec{p}-\vec{p}'+\vec{Q}|^{-2}$$

$$\times(n,p+k|e^{i\vec{Q}\cdot\vec{r}_1}|l,p'+k)(mp'|e^{-i\vec{Q}'\cdot\vec{r}_{1'}}|np)\,\mathcal{P}[\varepsilon_l(p'+k)-\varepsilon_m(p')-\varepsilon]^{-1}$$

$$\times\Big(f(\varepsilon_l(p'+k))\,\mathrm{Re}\,\epsilon^{-1}(p-p',Q,Q';\varepsilon_l(p'+k)-\varepsilon_n(p+k))$$

$$-f(\varepsilon_m(p'))\,\mathrm{Re}\,\epsilon^{-1}(p-p',Q,Q';\varepsilon_m(p')-\varepsilon_n(p'))$$

$$-\mathcal{P}\pi^{-1}\int_{-\infty}^{0}\mathrm{Im}\,\epsilon^{-1}(p-p',Q,Q';x)\{[\varepsilon_m(p')-\varepsilon_{n'}(p)-x]^{-1}-[\varepsilon_l(p'+k)-\varepsilon_n(p+k)-x]^{-1}\}dx\Big)$$

$$\times\mathcal{P}\Gamma^E_{J,lm}(p',k;\varepsilon_{n'}(p),\varepsilon_n(p+k),\varepsilon)\ . \tag{5.4}$$

The dominant contributions to Eq. (5.4) can now be estimated in the manner used by Weiner. He assumed that Γ^E_J was a slowly varying function of p', and could be removed from the integration and evaluated at $p'=p$. The integral equation was then solved approximately. In addition, the off-diagonal ($Q\neq Q'$) components of ϵ^{-1}, associated with local field corrections may be ignored. Because of the singular nature of the Coulomb denominators, we can choose $Q=0$ for the most important contribution. As a consequence, $m=n'$ and $l=n$ yield the maximum contribution for the product of matrix elements. These approximations give

$$\mathcal{P}\Gamma^E_{J,nn'}(p,k;\varepsilon_{n'}(p),\varepsilon_n(p+k),\varepsilon)\simeq\Gamma^0_{J,nn'}(p,k)\Big(1-\Omega^{-1}\textstyle\sum_{p'}e^2|\vec{p}-\vec{p}'|^{-2}$$

$$\times(n,p+k|n,p'+k)(n'p'|n'p)\{f(\varepsilon_{n'}(p'))\,[\varepsilon_n(p'+k)-\varepsilon_{n'}(p')-\varepsilon]^{-1}$$

$$\times\mathrm{Re}\,\epsilon^{-1}(p-p',0,0;\varepsilon_{n'}(p')-\varepsilon_{n'}(p))$$

$$+\mathcal{P}\pi^{-1}\int_{-\infty}^{0}\mathrm{Im}\,\epsilon^{-1}(p-p',0,0;x)[\varepsilon_{n'}(p)-\varepsilon_{n'}(p)-x]^{-1}[\varepsilon_n(p'+k)-\varepsilon_n(p+k)-x]^{-1}dx\}\Big)\ . \tag{5.5}$$

Because $\varepsilon_{n'}(p')-\varepsilon_{n'}(p)$ vanishes as $|\vec{p}-\vec{p}'|$ when $|\vec{p}-\vec{p}'|\to 0$ then

$$\mathrm{Re}\,\epsilon^{-1}(p-p',0,0;\varepsilon_{n'}(p')-\varepsilon_{n'}(p))$$

can be replaced by $\mathrm{Re}\,\epsilon^{-1}(p-p',0,0;0)$. Moreover, the principal contribution to $\mathrm{Im}\,\epsilon^{-1}(p-p',0,0;x)$ for $|p-p'|<q_c$, the cutoff wave vector, is that due to plasmon excitation; that small part due to pair excitations is smoothly varying, yielding, on the average, a nearly vanishing result. Also, $(n,p+k|n,p'+k)\approx 1$ and $(n'p'|n'p)\approx 1$ for most p,p' of interest. Consequently, using Eq. (4.15) we obtain

$$\mathcal{P}\Gamma^{E}_{J,nn'}(p,k;\varepsilon_{n'}(p),\varepsilon_n(p+k),\varepsilon)\simeq\Gamma^{0}_{J,nn'}(p,k)[1-\alpha_{nn'}(p,k;\varepsilon)]^{-1}\quad, \tag{5.6}$$

in which

$$\alpha_{nn'}(p,k;\varepsilon)=\Omega^{-1}|\bar{M}|^2\textstyle\sum_{p'}e^2|\vec{p}-\vec{p}'|^{-2}\{f(\varepsilon_{n'}(p'))\mathrm{Re}\,\epsilon^{-1}(p-p',0,0;0)$$
$$+\tfrac{1}{2}\varepsilon_P[\varepsilon_{n'}(p')-\varepsilon_{n'}(p)+\varepsilon_P]^{-1}[\varepsilon_n(p'+k)-\varepsilon_n(p+k)+\varepsilon_P]^{-1}\}\quad. \tag{5.7}$$

$|\bar{M}|^2$ is an average of the product $(n,p+k|n,p'+k)(n'p'|n'p)$ over the p and p' for which the maximum contribution to $\alpha_{nn'}(p,k;\varepsilon)$ is made. The two terms in Eq. (5.7) correspond to the two terms in Eq. (2.10); Mahan's[10] results are obtained when Eq. (5.6) is expanded to first order in $\alpha_{nn'}(p,k;\varepsilon)$.

If p is not too far from the Fermi momentum, $\alpha_{n'}(p)$, $\alpha_n(p+k)$, and $\alpha_{nn'}(p,k;\varepsilon)$, given, respectively, by Eqs. (4.17) and (5.7), are not only slowly varying in magnitude but also contain similar matrix elements, energy denominators, and ranges of integration which make their values almost identical. Upon substituting the first two into the expressions for the spectral densities and the third in the expression for the vertex function, we find that Eq. (3.33) becomes

$$\mathrm{Im}\,\chi^{T}_{JJ}(k,0,0;\omega)\simeq\tfrac{1}{3}\Omega^{-1}\sum_{P}\sum_{n,n'}|\Gamma^{0}_{J,nn'}(p,k)|^2[1-\alpha_{nn'}(p,k;\varepsilon)]^2$$
$$\times[1+\alpha_{n'}(p)]^{-1}[1+\alpha_n(p+k)]^{-1}|\epsilon_E^{-1}(k,Q_{nn'},Q_{nn'};\omega)|^{-2}$$
$$\times[f(\varepsilon_{n'}(p))-f(\varepsilon_n(p+k))]\,\delta(\varepsilon_n(p+k)-\varepsilon_{n'}(p)-\varepsilon)\quad. \tag{5.8}$$

Consequently, significant cancellation between the spectral density and vertex-function terms occurs. The net enhancement of the absorption due to many-body effects is small. In fact, because of the screening factor, the absorption may be reduced.

VI. HIGHER-ORDER PROCESSES

In this section, the two processes necessary to guarantee a conserving approximation are considered. The magnitude of their net contribution is crudely estimated, but in any case found to be negligible. The comments of the last section concerning Mahan's[10] and Weiner's[14] calculations suggest that the magnitude of the correction to Γ^{0}_{J} associated with the first iteration of Eq. (5.2) is satisfactory for an estimate of the magnitude of the true Γ^{E}_{J}. The influence of the two screened Coulomb scattering processes will be estimated similarly by replacing Γ^{E}_{J} with Γ^{0}_{J}. In addition, the propagator given by Eq. (4.11) will be used.

The manipulations are fairly straightforward, albeit complicated. They yield, for the first term in the square brackets of Eq. (5.2),

$$(\varepsilon_l-\varepsilon_m-\omega_\mu)^{-1}\{(f_l-f_{\bar{l}})(\omega_\nu+\omega_\mu+\varepsilon_{\bar{l}}-\varepsilon_l-\varepsilon_{\bar{m}})^{-1}[\mathcal{P}\pi^{-1}\textstyle\int_{-\infty}^{+\infty}\tfrac{1}{2}(\coth\tfrac{1}{2}\beta x)\,\mathrm{Im}\,\epsilon^{-1}(;x)$$
$$\times\tilde{\epsilon}^{-1}(;x+\omega_\mu)(x-\omega_\nu+\varepsilon_m)^{-1}dx+\mathcal{P}\pi^{-1}\textstyle\int_{-\infty}^{+\infty}\tfrac{1}{2}(\coth\tfrac{1}{2}\beta x)\tilde{\epsilon}^{-1}(;x-\omega_\mu)\,\mathrm{Im}\,\epsilon^{-1}(;x)$$
$$\times(x-\omega_\nu-\omega_\mu+\varepsilon_{\bar{m}})^{-1}dx+\tilde{\epsilon}^{-1}(;\omega_\nu-\varepsilon_{\bar{m}})\tilde{\epsilon}^{-1}(;\omega_\nu+\omega_\mu-\varepsilon_{\bar{m}})\tfrac{1}{2}\tanh\tfrac{1}{2}\beta\varepsilon_{\bar{m}}$$
$$-\mathcal{P}\pi^{-1}\textstyle\int_{-\infty}^{+\infty}\tfrac{1}{2}(\coth\tfrac{1}{2}\beta x)\,\mathrm{Im}\epsilon^{-1}(;x)\tilde{\epsilon}^{-1}(;x+\omega_\mu)(x+\omega_\mu+\varepsilon_l-\varepsilon_{\bar{l}})^{-1}dx$$
$$-\mathcal{P}\pi^{-1}\textstyle\int_{-\infty}^{+\infty}\tfrac{1}{2}(\coth\tfrac{1}{2}\beta x)\tilde{\epsilon}^{-1}(;x-\omega_\mu)\,\mathrm{Im}\epsilon^{-1}(;x)(x+\varepsilon_{\bar{l}}-\varepsilon_l)^{-1}dx$$
$$-\tilde{\epsilon}^{-1}(;\varepsilon_l-\varepsilon_{\bar{l}}-\omega_\mu)\,\mathrm{Re}\,\epsilon^{-1}(;\varepsilon_{\bar{l}}-\varepsilon_l)\tfrac{1}{2}\coth\beta(\varepsilon_{\bar{l}}-\varepsilon_l)]$$
$$-(f_m-f_{\bar{l}})(\omega_\nu+\varepsilon_{\bar{l}}-\varepsilon_m-\varepsilon_{\bar{m}})^{-1}[\mathcal{P}\pi^{-1}\textstyle\int_{-\infty}^{+\infty}\tfrac{1}{2}(\coth\tfrac{1}{2}\beta x)\,\mathrm{Im}\,\tilde{\epsilon}^{-1}(;\omega_\nu-\varepsilon_m)\,\mathrm{Im}\,\epsilon^{-1}(;x+\omega_\mu)$$
$$\times(x-\omega_\nu+\varepsilon_{\bar{m}})^{-1}dx+\mathcal{P}\pi^{-1}\textstyle\int_{-\infty}^{+\infty}\tfrac{1}{2}(\coth\tfrac{1}{2}\beta x)\tilde{\epsilon}^{-1}(;x-\omega_\mu)\,\mathrm{Im}\,\epsilon^{-1}(;x)(x-\omega_\nu-\omega_\mu+\varepsilon_{\bar{m}})^{-1}$$
$$+\tilde{\epsilon}^{-1}(;\omega_\nu-\varepsilon_{\bar{m}})\tilde{\epsilon}^{-1}(;\omega_\nu+\omega_\mu-\varepsilon_{\bar{m}})\tfrac{1}{2}\tanh\tfrac{1}{2}\beta\varepsilon_{\bar{m}}-\mathcal{P}\pi^{-1}\textstyle\int_{-\infty}^{+\infty}\tfrac{1}{2}(\coth\tfrac{1}{2}\beta x)$$
$$\times\mathrm{Im}\,\epsilon^{-1}(;x)\tilde{\epsilon}^{-1}(;x+\omega_\mu)(x+\varepsilon_{\bar{l}}-\varepsilon_m)^{-1}dx-\mathcal{P}\pi^{-1}\textstyle\int_{-\infty}^{+\infty}\tfrac{1}{2}(\coth\tfrac{1}{2}\beta x)$$
$$\times\tilde{\epsilon}^{-1}(;x)(x-\omega_\mu+\varepsilon_{\bar{l}}-\varepsilon_m)^{-1}dx-\mathrm{Re}\,\epsilon^{-1}(;\varepsilon_{\bar{l}}-\varepsilon_m-\omega_\mu)\tilde{\epsilon}^{-1}(;\varepsilon_{\bar{l}}-\varepsilon_m-\omega_\mu)\tfrac{1}{2}\coth\tfrac{1}{2}\beta(\varepsilon_{\bar{l}}-\varepsilon_m)]\}\quad, \tag{6.1}$$

exclusive of all factors involving matrix elements, Coulomb interactions, and summations over momentum

variables and band indices.

The momentum variables in $\tilde{\epsilon}^{-1}$ and ϵ^{-1} are implicit. For simplicity, f_l denotes $f(\varepsilon_l)$ and ε_l signifies $(\varepsilon_l(p'))$, consistent with the notation of Eq. (5.2). Energy denominators are, if necessary, principal parts about those points at which they vanish. An expression similar to that in Eq. (6.1) is obtained for the second term in square brackets in Eq. (5.2).

Conversion of the cotangent terms into Fermi factors, employment of Eq. (3.16), and a lengthy rearrangement procedure yield finally

$$
\begin{aligned}
&\mathcal{P}\pi^{-1}\int_{-\infty}^{+\infty}\left[\tfrac{1}{2}f_m f_l(1-f_{\bar{l}})(\coth\tfrac{1}{2}\beta x+1)-\tfrac{1}{2}(1-f_m)(1-f_l)f_{\bar{l}}(\coth\tfrac{1}{2}\beta x-1)\right]\\
&\times[\mathrm{Im}\epsilon^{-1}(;x)\tilde{\epsilon}^{-1}(;x+\omega_\mu)(x+\varepsilon_{\bar{m}}-\omega_\mu)^{-1}(x+\omega_\mu+\varepsilon_{\bar{l}}-\varepsilon_l)^{-1}(x+\varepsilon_{\bar{l}}-\varepsilon_m)^{-1}\\
&+\tilde{\epsilon}^{-1}(;x-\omega_\mu)\,\mathrm{Im}\,\epsilon^{-1}(;x)(x+\varepsilon_{\bar{m}}-\omega_\nu-\omega_\mu)^{-1}(x+\varepsilon_{\bar{l}}-\varepsilon_l)^{-1}(x+\varepsilon_{\bar{l}}-\varepsilon_m-\omega_\mu)^{-1}]\,dx\\
&+(\varepsilon_l-\varepsilon_m-\omega_\mu)^{-1}\{\mathcal{P}\pi^{-1}\int_{-\infty}^{+\infty}[\tfrac{1}{2}(1-f_m)f_l(1-f_{\bar{l}})(\coth\tfrac{1}{2}\beta x+1)-\tfrac{1}{2}f_m(1-f_l)f_{\bar{l}}\\
&\times(\coth\tfrac{1}{2}\beta x-1)][\mathrm{Im}\,\epsilon^{-1}(;x)\tilde{\epsilon}^{-1}(;x+\omega_\mu)(x+\varepsilon_{\bar{m}}-\omega_\nu)^{-1}(x+\omega_\mu+\varepsilon_{\bar{l}}-\varepsilon_l)^{-1}\\
&+\epsilon^{-1}(;x-\omega_\mu)\,\mathrm{Im}\,\epsilon^{-1}(;x)(x-\omega_\nu-\omega_\mu+\varepsilon_{\bar{m}})^{-1}(x+\varepsilon_l-\varepsilon_{\bar{l}})^{-1}]\,dx\}-\mathcal{P}\pi^{-1}\int_{-\infty}^{+\infty}[\tfrac{1}{2}f_m(1-f_l)(1-f_{\bar{l}})\\
&\times(\coth\tfrac{1}{2}\beta x+1)-\tfrac{1}{2}(1-f_m)f_l f_{\bar{l}}(\coth\tfrac{1}{2}\beta x-1)][\mathrm{Im}\,\epsilon^{-1}(;x)\tilde{\epsilon}^{-1}(;x+\omega_\mu)(x+\varepsilon_{\bar{m}}-\omega_\nu)^{-1}\\
&\times(x+\varepsilon_{\bar{l}}-\varepsilon_m)^{-1}+\tilde{\epsilon}^{-1}(;x+\omega_\mu)\,\mathrm{Im}\,\epsilon^{-1}(;x)(x-\omega_\nu-\omega_\mu+\varepsilon_{\bar{m}})^{-1}(x+\varepsilon_{\bar{l}}-\varepsilon_m-\omega_\mu)^{-1}]\,dx\\
&+\{[f_m(1-f_l)f_{\bar{l}}+(1-f_m)f_l(1-f_{\bar{l}})](\omega_\nu+\varepsilon_l+\varepsilon_m-\varepsilon_{\bar{m}})^{-1}\\
&-[f_l(1-f_{\bar{l}})f_{\bar{m}}+(1-f_l)f_{\bar{l}}(1-f_{\bar{m}})]\;(\omega_\nu+\omega_\mu+\varepsilon_{\bar{l}}-\varepsilon_l-\varepsilon_{\bar{m}})^{-1}\}\tilde{\epsilon}^{-1}(;\omega_\nu-\varepsilon_{\bar{m}})\tilde{\epsilon}^{-1}(;\omega_\nu+\omega_\mu-\varepsilon_{\bar{m}})\quad .
\end{aligned}
\tag{6.2}
$$

To find $\mathcal{P}\Gamma_J$, we used the appropriate analytic-continuation procedure which amounts to replacing $\omega_\nu+\omega_\mu$ by $\varepsilon_n(p+k)$, ω_ν by $\varepsilon_{n'}(p)$, ω_μ by ε, and all integrals containing energy denominators by principal-parts integrations. Letting $T\to 0$ [in order to use Eq. (3.36)] and introducing the Coulomb factors, matrix elements and, summations over momentum variables and band indices, yields

$$
\begin{aligned}
&\Omega^{-2}\sum_{p',q}\sum_{m,l,\bar{m},\bar{l}}\sum_{Q,Q',\bar{Q},\bar{Q}'}(n,p+k|e^{i\vec{\bar{Q}}\cdot\vec{r}_1}|\bar{m},p-q)(\bar{m},p-q|e^{-i\vec{Q}'\cdot\vec{r}_1}|n'p)(mp'|e^{i\vec{Q}\cdot\vec{r}_3}|\bar{l},p'-q)\\
&\times(\bar{l},p'-q|e^{-i\vec{\bar{Q}}'\cdot\vec{r}_3}|l,p'+k)e^4|\vec{q}+\vec{k}+\vec{\bar{Q}}|^{-2}|\vec{q}+\vec{Q}|^{-2}(\{\mathcal{P}\pi^{-1}\int_{-\infty}^{+\infty}[\theta(x)f_m f_l(1-f_{\bar{l}})\\
&+\theta(-x)(1-f_m)(1-f_l)f_{\bar{l}}][\mathrm{Im}\,\epsilon^{-1}(;x)\,\mathrm{Re}\,\epsilon^{-1}(;x+\omega)(x+\varepsilon_{\bar{m}}-\varepsilon_n)^{-1}(x+\varepsilon+\varepsilon_{\bar{l}}-\varepsilon_l)^{-1}\\
&\times(x+\varepsilon_{\bar{l}}-\varepsilon_m)^{-1}+\mathrm{Re}\,\epsilon^{-1}(;x-\omega)\,\mathrm{Im}\,\epsilon^{-1}(;x)(x+\varepsilon_{\bar{m}}-\varepsilon_n)^{-1}(x+\varepsilon_{\bar{l}}-\varepsilon_l)^{-1}(x+\varepsilon_{\bar{l}}-\varepsilon_m-\varepsilon)^{-1}]\,dx\}\\
&+(\varepsilon_l-\varepsilon_m-\varepsilon)^{-1}\{\mathcal{P}\pi^{-1}\int_{-\infty}^{+\infty}[\theta(x)(1-f_m)f_l(1-f_{\bar{l}})+\theta(-x)f_m(1-f_l)f_{\bar{l}}][\mathrm{Im}\epsilon^{-1}(;x)\\
&\times\mathrm{Re}\,\epsilon^{-1}(;x+\omega)(x+\varepsilon_{\bar{m}}-\varepsilon_{n'})^{-1}(x+\varepsilon+\varepsilon_{\bar{l}}-\varepsilon_l)^{-1}+\mathrm{Re}\epsilon^{-1}(;x-\omega)\mathrm{Im}\epsilon^{-1}(;x)(x+\varepsilon_{\bar{m}}-\varepsilon_n)^{-1}\\
&\times(x+\varepsilon_{\bar{l}}-\varepsilon_l)^{-1}]dx\}-\mathcal{P}\pi^{-1}\int_{-\infty}^{+\infty}[\theta(x)f_m(1-f_l)(1-f_{\bar{l}})+\theta(-x)(1-f_m)f_l f_{\bar{l}}]\\
&\times[\mathrm{Im}\,\epsilon^{-1}(;x)\,\mathrm{Re}\,\epsilon^{-1}(;x+\omega)(x+\varepsilon_{\bar{m}}-\varepsilon_{n'})^{-1}(x+\varepsilon_{\bar{l}}-\varepsilon_m)^{-1}+\mathrm{Re}\,\epsilon^{-1}(;x-\omega)\,\mathrm{Im}\,\epsilon^{-1}(;x)\\
&\times(x+\varepsilon_{\bar{m}}-\varepsilon_n)^{-1}(x+\varepsilon_{\bar{l}}-\varepsilon_m-\varepsilon)^{-1}]\,dx+\{[f_m(1-f_l)f_{\bar{m}}+(1-f_m)f_l(1-f_{\bar{m}})]\\
&\times(\varepsilon_{n'}+\varepsilon_{\bar{l}}-\varepsilon_m-\varepsilon_{\bar{m}})^{-1}-[f_l(1-f_{\bar{l}})f_{\bar{m}}+(1-f_l)f_{\bar{l}}(1-f_{\bar{m}})](\varepsilon_n+\varepsilon_{\bar{l}}-\varepsilon_l-\varepsilon_{\bar{m}})^{-1}\}\\
&\times\mathrm{Re}\,\epsilon^{-1}(;\varepsilon_{n'}-\varepsilon_{\bar{m}})\,\mathrm{Re}\,\epsilon^{-1}(;\varepsilon_n-\varepsilon_{\bar{m}}))\,\Gamma^0_{J,lm}(p',k)\quad .
\end{aligned}
\tag{6.3}
$$

Of the many terms to be evaluated, the most important may be expected to couple only transitions between bands n and n'. Thus m may be set equal to n' and l to n. It is also plausible to assume that substantial contributions will occur for those values of momenta and band indices which tend to make the Coulomb terms singular and the product of matrix elements as large as possible. Thus, setting $Q=Q'=\bar{Q}=\bar{Q}'$ implies that for a non-negligible contribution $\bar{m}$ and $\bar{l}$ should take on the value n or n'.

As an illustration of the procedure used to estimate the terms, let $\bar{m}=n'$ and $\bar{l}=n$. Upon setting the photon momentum $\hbar k=0$, this yields

$$\Omega^{-2}\sum_{p,q}(n,p|\,n',p-q)(n',p-q|n',p)(n',p'|n,p'-q)(n,p'-q|n,p')e^4|q|^{-4}\Gamma^0_{J,nn'}(p',0)$$
$$\times\big(f(\varepsilon_{n'}(p'))[\varepsilon_n(p')-\varepsilon_{n'}(p')-\varepsilon]^{-1}\mathcal{P}\pi^{-1}\int_0^\infty\{\operatorname{Im}\epsilon^{-1}(q;x)\operatorname{Re}\epsilon^{-1}(q;x+\omega)$$
$$\times[x+\varepsilon_{n'}(p-q)-\varepsilon_n(p)]^{-1}[x+\varepsilon_n(p'-q)-\varepsilon_{n'}(p')]^{-1}+\operatorname{Re}\epsilon^{-1}(q;x-\omega)\operatorname{Im}\epsilon^{-1}(q;x)$$
$$\times[x+\varepsilon_{n'}(p-q)-\varepsilon_n(p)]^{-1}[x+\varepsilon_n(p'-q)-\varepsilon_{n'}(p')-\varepsilon]^{-1}\}\,dx+f(\varepsilon_{n'}(p-q))$$
$$\times[\varepsilon_{n'}(p)+\varepsilon_n(p'-q)-\varepsilon_{n'}(p')-\varepsilon_{n'}(p-q)]^{-1}\operatorname{Re}\epsilon^{-1}(q;\varepsilon_{n'}(p)-\varepsilon_{n'}(p-q))$$
$$\times\operatorname{Re}\epsilon^{-1}(q;\varepsilon_n(p)-\varepsilon_{n'}(p-q))\big)\ . \tag{6.4}$$

In the first term, the significant contribution should be that associated with the plasmon part of $\operatorname{Im}\epsilon^{-1}$, which is largest for $q=0$. Plasmon excitations corresponding to finite q in the square bracket will be approximated by their $q=0$ form. The errors that are thereby introduced may be expected to be reasonably small because, as the plasma peak is broadened and becomes smaller due to interband excitations, there is a compensating effect arising from the smaller-energy denominators.[28]

With these approximations the integral of the term in square brackets assumes the form

$$-\mathcal{P}\pi^{-1}\int_0^\infty[\operatorname{Im}\epsilon^{-1}(0;x)\operatorname{Re}\epsilon^{-1}(0;x)\,x^{-1}(x+\varepsilon_n(p')-\varepsilon_{n'}(p'))^{-1}$$
$$+\operatorname{Re}\epsilon^{-1}(0;x-\omega)\operatorname{Im}\epsilon^{-1}(0;x)(x-\varepsilon)^{-1}(x-\varepsilon+\varepsilon_n(p')-\varepsilon_{n'}(p'))^{-1}]\,dx\ , \tag{6.5}$$

which becomes, with the help of Eq. (4.15),

$$\tfrac{1}{2}\varepsilon_P\{\operatorname{Re}\epsilon^{-1}(0;\omega_P+\omega)\varepsilon_P^{-1}[\varepsilon_P+\varepsilon_n(p')-\varepsilon_{n'}(p')]^{-1}$$
$$+\operatorname{Re}\epsilon^{-1}(0;\omega_P-\omega)[\varepsilon_P-\varepsilon]^{-1}[\varepsilon_P-\varepsilon+\varepsilon_n(p')-\varepsilon_{n'}(p')]^{-1}\}\ . \tag{6.6}$$

Observe that the first term in the square bracket corresponds to that given by Eq. (2.11) and (2.12) determined by the phenomenological Hamiltonian.

At or near the threshold, $\Gamma^0_{J,nn'}$ will be largest (in an alkali metal) and $[\varepsilon_n(p')-\varepsilon_{n'}(p')-\varepsilon]^{-1}$ nearly singular for $p'\approx p$. Hence, choose $p=p'$ in Eq. (6.4), let $q=0$ and assume that $\varepsilon<\varepsilon_P$. Also, let $\operatorname{Re}\epsilon^{-1}$ be approximated by the corresponding expression from the Lindhard dielectric function

$$\operatorname{Re}\epsilon^{-1}(0;\omega_P\pm\omega)\approx\{1-[\varepsilon_P/(\varepsilon_P+\varepsilon)]^2\}^{-1}\ . \tag{6.7}$$

The expression (6.6) then becomes

$$\varepsilon_P/(4\varepsilon_P^2-\varepsilon^2)\ . \tag{6.8}$$

The magnitude of the second term of (6.4) is limited by the Fermi-factor restrictions $\varepsilon_{n'}(p-q)<0$, $\varepsilon_{n'}(p')<0$, $\varepsilon_{n'}(p)<0$, and $\varepsilon_n(p'-q)>0$. For fixed p, and most q, $\varepsilon_{n'}(p)-\varepsilon_{n'}(p-q)>0$ and $\varepsilon_n(p'-q)-\varepsilon_{n'}(p')\gtrsim\varepsilon$ so that q can be set equal to zero. Furthermore the dielectric functions appearing in this term may be regarded as slowly varying functions of q. This gives

$$f(\varepsilon_{n'}(p-q))[\varepsilon_n(p')-\varepsilon_{n'}(p')]^{-1}\operatorname{Re}\epsilon^{-1}(q,0,0;0)\operatorname{Re}\epsilon^{-1}(q,0,0;\omega)\ .$$

Using the Thomas-Fermi approximation, $\operatorname{Re}\epsilon^{-1}(q,0,0;0)\simeq|q|^2/(|q|^2+k_{\mathrm{TF}}^2)$ (where k_{TF} is the Thomas-Fermi wave vector) and observing that the second term has a Fermi-function restriction which the first does not, it can be seen that for most q, the plasmon term dominates. Returning to expression (6.4), then it is found to be

$$\Omega^{-2}\sum_{p',q}(n,p|n',p-q)(n',p-q|n',p)(n',p'|n,p'-q)(n,p'-q|n,p')e^4|q|^{-4}\Gamma^0_{J,nn'}(p,k)$$
$$\times f(\varepsilon_{n'}(p'))[\varepsilon_n(p')-\varepsilon_{n'}(p')-\varepsilon]^{-1}\varepsilon_P(4\varepsilon_P^2-\varepsilon^2)^{-1}\ . \tag{6.9}$$

For small q

$$(n,p'-q|n,p')\simeq1,\ (n',p-q|n',p)\simeq1\ ,\quad (n,p|n',p-q)\simeq-(e)^{-1}\vec{q}\cdot\vec{\Gamma}^0_{J,nn'}(p,0)/\varepsilon_{nn'}(p)\ ,$$
$$(n',p'|n,p'-q)\simeq(e)^{-1}\vec{q}\cdot\vec{\Gamma}^0_{J,nn'}(p',0)/\varepsilon_{nn'}(p')\ .$$

By assuming that the product of matrix elements and one Coulomb factor $e^2|q|^{-2}$ is slowly varying with q, it is possible to write

$$-\Omega^{-1}\sum_{p'} f(\varepsilon_{n'}(p'))[\varepsilon_{nn'}(p')\varepsilon_{nn'}(p)]^{-1}\varepsilon_P(4\varepsilon_P^2-\varepsilon^2)^{-1}[\varepsilon_n(p')-\varepsilon_{n'}(p')-\varepsilon]^{-1}$$
$$\times\Omega^{-1}\sum_q[\vec{q}\cdot\vec{\Gamma}^0_{J,nn'}(p,0)][\vec{q}\cdot\vec{\Gamma}^0_{J,nn'}(p,0)]^* e^2|q|^{-4}\Gamma^0_{J,nn'}(p,0) \quad . \tag{6.10}$$

With a q integration ranging through a sphere with a radius on the order of q_c, it is readily shown that (6.10) becomes

$$-\Omega^{-1}\sum_{p'} f(\varepsilon_{n'}(p'))[\varepsilon_{nn'}(p')\varepsilon_{nn'}(p)]^{-1}\varepsilon_P(4\varepsilon_P^2-\varepsilon^2)^{-1}[\varepsilon_n(p')-\varepsilon_{n'}(p')-\varepsilon]^{-1}$$
$$\times(e^2 q_c/4\pi)\tfrac{1}{3}\vec{\Gamma}^0_{J,nn'}(p,0)\cdot\vec{\Gamma}^{0*}_{J,nn'}(p',0)\Gamma^0_{J,nn'}(p,0) \quad . \tag{6.11}$$

Since $p'\approx p$ is the most important part of the integration range, we write instead

$$-\{\Omega^{-1}\sum_{p'} f(\varepsilon_{n'}(p'))\tfrac{1}{3}|\Gamma^0_{J,nn'}(p',0)|^2[\varepsilon_n(p')-\varepsilon_{n'}(p')-\varepsilon]^{-1}[\varepsilon-\varepsilon_{nn'}(p')]^{-1}$$
$$\times\varepsilon_P(4\varepsilon_P^2-\varepsilon^2)^{-1}(e^2 q_c/4\pi)\}\,\Gamma^0_{J,nn'}(p,0) \quad ; \tag{6.12}$$

$\varepsilon_{nn'}(p)=\varepsilon$ has been used because the final calculation of the absorption contains a delta function $\delta(\varepsilon_n(p+k)-\varepsilon_{n'}(p)-\varepsilon)$. If for the momentum k and energy ε, the main contribution to $\mathrm{Re}\,\chi^{0T}_{JJ}(k,0,0;\omega)$ comes from the virtual transitions between bands n' and n, then the final result is roughly

$$-\mathrm{Re}\,\chi^0_{J\,J}{}^T(k;\omega)(e^2 q_c/4\pi\varepsilon_P)\varepsilon_P^2(4\varepsilon_P^2-\varepsilon^2)^{-1}\langle\varepsilon/\varepsilon_{nn'}(p')\rangle\Gamma^0_{J,nn'}(p,0)\,, \tag{6.13}$$

where $\langle\,\rangle$ represents some average over allowed p. The evaluation of the remaining significant terms in (6.3) follows along the above lines and yields one term nearly identical to (6.13) and two terms nearly identical with (6.13) except that $\varepsilon_P^2(4\varepsilon_P^2-\varepsilon^2)^{-1}$ is replaced by $\frac{1}{2}(2\varepsilon_P^2-\varepsilon^2)(4\varepsilon_P^2-\varepsilon^2)^{-1}$. Adding up all four gives

$$-\mathrm{Re}\,\chi^{0T}_{JJ}(k,\omega)\langle\varepsilon/\varepsilon_{nn'}(p)\rangle(e^2 q_c/4\pi\varepsilon_P)\Gamma^0_{J,nn'}(p,0) \quad . \tag{6.14}$$

We recall that the corresponding correction to $\Gamma^0_{J,nn'}(p,k)$ from the single-screened scattering process was approximately $\alpha\Gamma^0_{J,nn'}$, where $\alpha=e^2 q_c/4\pi^2\varepsilon_P$ so that the additional correction is scaled down by two extra factors. The second $\langle\varepsilon/\varepsilon_{nn'}(p)\rangle$ is less than 1 near the threshold and the first $\mathrm{Re}\,\chi^{0T}_{JJ}$ can be estimated as ~ 0.1 for Na using Butcher's[29] model for the band structure.

However, the final result is even smaller, since, if the same analysis, procedures and approximations discussed here are used for evaluating the corresponding contribution from the second term in the square brackets of Eq. (5.2), then the contribution is roughly given by the negative of (6.14). Consequently, the net effect of the two processes is seen to yield a small correction which we estimate to be of order 0.01.

VII. NEW CALCULATIONS WITHIN THE RPA

The calculations and discussions of the previous sections provide strong evidence that the influence of electron-electron interactions is not sufficient to explain the substantial discrepancies existing between the experimental data and theoretical estimates of the optical absorption, particularly for aluminum. This suggests that a careful reexamination of the RPA numerical calculations be undertaken in order to ascertain whether a resolution of the discrepancies within its framework might eliminate the difficulties.

Heretofore, for aluminum, the most thorough investigation on that basis was that of Ehrenreich, Philipp, and Segall.[4] They used a band structure based upon a two pseudopotential and effective-mass parameter fit to energy eigenvalues determined by the Korringa-Kohn-Rostoker (KKR) method.[30] The quantities chosen were the pseudopotential parameters $V_{111}=0.313$ eV, $V_{200}=0.585$ eV, and effective mass $m^*=1.03$ m. Their momentum matrix elements were evaluated explicitly at only a few points because of the complexity of the KKR scheme. For the other points in the zone, an interpolation method was used. In particular, for their calculation, which we designate as EPSI, the principal contributions to the absorption peak come from transitions at W and in the (001) plane containing the Σ axis. At W, the momentum matrix element, in units of $2\pi/a$ was estimated as 0.491 and for Σ, at the point $(\frac{5}{8},\frac{5}{8},0)(2\pi/a)$, it was given by 0.421. The Σ transitions gave the predominant contribution to the absorption peak. The total contribution to the sum rule, Eq. (1.1), fell short of the expected experimental values by about a factor of 3.

In Ref. 4, ϵ_2 was first derived from the available reflectivity data. Then, a two-parameter Drude model was used to match the intraband absorption at infrared energies. By subtraction from the total ϵ_2, the interband part was obtained. Reasonable Drude-model fits to the intraband region with different values of the parameters can be found, but they do not significantly alter the structure of the interband absorption.

Subsequent to that work, Ashcroft[31] attempted to match Fermi-structure data with a pseudopotential band structure. He found that $V_{111} = 0.243$ eV and $V_{200} = 0.762$ eV yielded the best fit to observed de Haas–van Alphen periods. The effective mass was an arbitrary scaling factor and could be chosen to match other data. For the resulting energy bands, there is no contribution at W to the absorption peak since the valence band of interest lies above the Fermi level. Thus, it might be expected that an RPA calculation of ϵ_2 would produce an even larger discrepancy between theory and experiment.

Calculations for this band structure were performed by Hughes *et al.*[19] and independently by the authors (denoted by AI) *using the pseudo-wave functions to determine the momentum matrix elements.* The results are illustrated in Fig. 9(a). It is seen that the agreement of the general features of the experimental and theoretical curves is far better than that obtained in EPSI; damping effects not included in these calculations might be expected to smooth the sharp theoretical structure. The reason for the coarseness of our absorption curve relative to that of Hughes *et al.*[19] is due to their use of a very high mesh density – 5×10^7 points throughout the whole zone – corresponding to about 100 times what we employed. Nevertheless, the results fundamentally corroborate one another. Our calculation of the interband contribution to the sum rule agrees within 10% with that estimated from the experimental data.[32]

In addition, we performed a similar calculation, denoted by EPSII, using the EPSI parameters. The results are compared with the previous calculation in Fig. 9(b). The essential difference produced was a shifting of the peak down from about 1.55 to about 1.25 eV; the contribution to the sum remained fundamentally unchanged. The shifting of the peak was not surprising, since a calculation just involving V_{200} and V_{111} in which V_{111} is relatively small yields energy differences for the energy bands of interest very close to $2V_{200}$. These have values 1.17 and 1.52 eV for the EPSII and AI calculations, respectively.

Why the EPSI calculation gave a peak near 1.5 eV is, therefore, not clear. But the more important aspect is the significant difference in the calculated magnitude of the absorption. The obvious source of this is the momentum matrix element which, for the EPSII calculation, had values 0.418 and 0.995, in units of $2\pi/a$, at the points $(1, \frac{1}{2}, 0)(2\pi/a)$ and $(\frac{5}{8}, \frac{5}{8}, 0)(2\pi/a)$, respectively. The large difference between EPSI and EPSII persists throughout the Σ region contributing to the peak. This is also true for the AI calculation which gives 0.997 at $(\frac{5}{8}, \frac{5}{8}, 0) \times (2\pi/a)$.

The question remains of whether the pseudo-wave functions are sufficient to give accurately the momentum matrix element. Previous calcula-

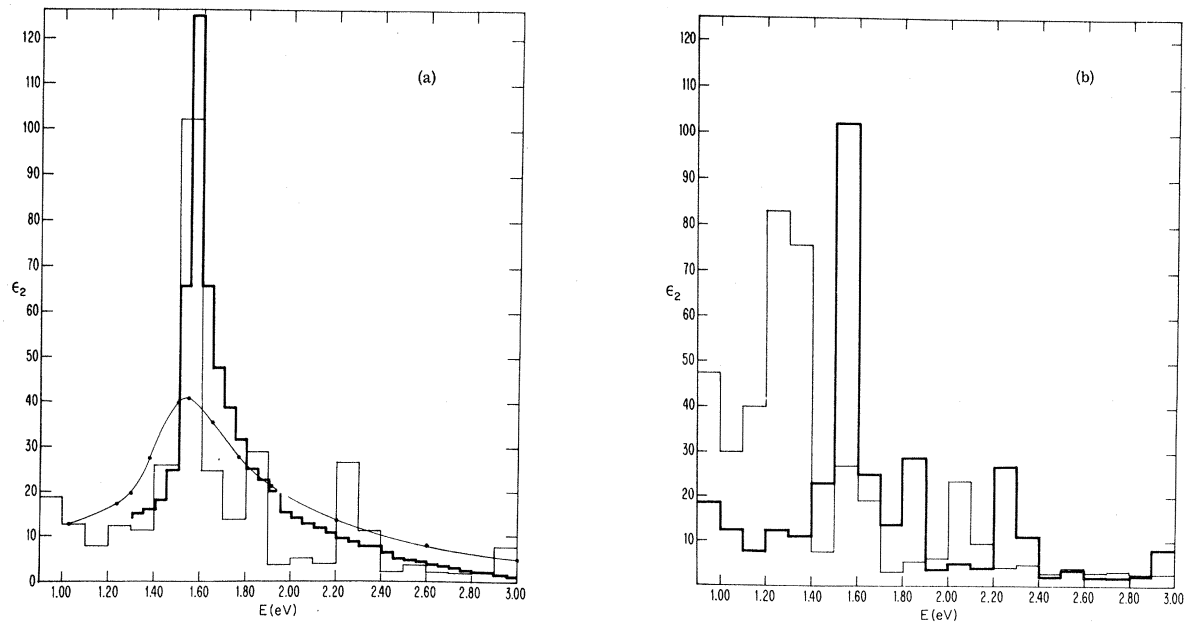

FIG. 9. (a) Histograms of the interband part of ϵ_2 for Al based on Ashcroft's parameters as calculated by Hughes *et al.* (heavy solid curve) and the authors (light solid curve) are compared with the experimental interband determination of Ref. 4. (b) Histogram of the interband part of ϵ_2 for Al based on Ashcroft's parameters (light solid curve) is compared with the based on Segall's parameters (heavy solid curve).

tions[7,8,12] leave the answer unclear. For sodium, Appelbaum[7] explicitly derived the true wave functions from the pseudo-wave functions and found a substantial *reduction* in the absorption – upwards of 80%. He used two pseudopotential parameters, V_{200} and V_{110}. It was then claimed by Overhauser,[8] apparently on the basis of a model calculation, that the suppression of the matrix element was due to nonorthogonality of the wave functions and if this error were corrected, there would be *no reduction* in the absorption. Animalu[12] considered Na and other alkali metals treating the lattice pseudopotential correctly to second order and taking into account the necessary core corrections. He found an *enhancement* of the matrix element by about 20% and of the absorption 50%.

There appears to be little physical distinction between the calculations of Appelbaum and Animalu except the relatively unimportant one that the latter used a nearly free-electron approach and the former does not. What may have produced the bulk of the difference was Appelbaum's inclusion of V_{200}. The work of Politzer *et al.*[33] suggests that the values of V_{200} which Appelbaum chose can produce substantial reduction (over 40%) of the matrix element which includes only the influence of V_{110}. Cutler[34] points out that inclusion of more plane waves may make the effect less severe.

The preceding discussion shows that it is important to determine the influence of introducing the true wave functions (as derived from the pseudo-wave functions). Rough estimates of ours based on Animalu's formalism suggested that such influence would be slight due to the small size of the aluminum core and the small ratio of band gap to absorption energy.

This was confirmed by detailed calculations for aluminum based on the formal expressions of Appelbaum. Our rederivation of his results yields an additional factor of $\frac{1}{2}$ in the function $B(k, k')$ given by his Eq. (10). Calculations were performed using both values of B with negligible difference. But if our expression is correct, then the reduction of the absorption in Appelbaum's work would probably be even more severe.

For aluminum we find that replacement of the pseudo-wave functions by the true wave functions reduces the momentum matrix element of interest by at most about 1% and often only a fraction of a percent. The wave functions used were found to be orthogonal to within about 10^{-3} and normalized to within 10^{-2} and often much less than that.

These results imply that our RPA results, AI, are probably sufficient to give a plausible corroboration of the optical absorption in aluminum. The reason for the discrepancy between the EPSI and EPSII estimates remains unclear, but it appears that the earlier calculations were subject to some error which we have been unable to trace.[35]

In sodium the situation remains far less clear than in aluminum. Aside from experimental difficulties that arise in working with such extremely oxidizable materials as the alkali metals, and which are now being resolved,[13] there are a number of theoretical difficulties that render calculations less reliable. First, the separation of ϵ_2 into inter- and intraband contributions is more difficult than in Al. Second, because the oscillator strength due to interband transitions is not localized in a small photon energy range as in Al, the conductivity sum rule cannot be used to check calculations. Third, for Na, as we have noted above, there remain many questions about the correct handling of calculations within the RPA especially with respect to the influence of core corrections and the various components of the lattice pseudopotential. Finally, the degree of cancellation between vertex corrections and dressing effects of the first-order electron-electron corrections is not known very well. This is, in part, due to inadequacies in the estimates of the correction factor $(1-\alpha)^{-1}$ which is more sensitive to the approximations made for sodium than for aluminum. This factor, which would be between the values given by Mahan[10] and Weiner,[14] is very large in sodium. Thus, for that material, cancellation occurs between two large quantities and hence the net result might still be substantial, even though this is not very probable. For aluminum, it is unlikely that it would be more than 10–20% at most.

ACKNOWLEDGMENTS

We are grateful to P. C. Martin for a number of illuminating discussions and to G. D. Mahan for reading a preliminary version of this manuscript. Helpful comments from T. Lubensky and V. O'Donnell are also appreciated.

---

*Work supported in part under Grant No. GP-8019 of the National Science Foundation and the Advanced Research Projects Agency.

[1]J. C. Phillips, in *Solid State Physics*, edited by F. Seitz and D. Turnbull (Academic, New York, 1966), Vol. 18, p. 56.

[2]E. O. Kane, Phys. Rev. 146, 558 (1966).
[3]G. Dresselhaus and M. S. Dresselhaus, Phys. Rev. 160, 649 (1967).
[4]H. Ehrenreich, H. R. Philipp, and B. Segall, Phys. Rev. 132, 1918 (1963).
[5]B. R. Cooper, H. Ehrenreich, and H. R. Philipp, Phys. Rev. 138, A494 (1965).
[6]F. M. Mueller and J. C. Phillips, Phys. Rev. 157, 600 (1967).
[7]J. Appelbaum, Phys. Rev. 144, 435 (1966).
[8]A. W. Overhauser, Phys. Rev. 156, 844 (1967).
[9]J. J. Hopfield, Phys. Rev. 139, A419 (1965).
[10]G. D. Mahan, Phys. Letters 24A, 708 (1967).
[11]G. D. Mahan, Phys. Rev. 153, 882 (1967).
[12]A. O. E. Animalu, Phys. Rev. 163, 557 (1967); 163, 562 (1967).
[13]N. Smith, Phys. Rev. Letters 21, 96 (1968).
[14]R. Weiner, Ph. D. thesis, Harvard University, 1967 (unpublished).
[15]That such cancellation occurs was pointed out to us by P. C. Martin (private communication).
[16]P. C. Martin and J. Schwinger, Phys. Rev. 115, 1342 (1959).
[17]G. Baym and L. P. Kadanoff, Phys. Rev. 124, 287 (1961).
[18]G. Baym, Phys. Rev. 127, 1391 (1962).
[19]A. J. Hughes, D. Jones, and A. H. Lettington, J. Phys. C 2, 102 (1969).
[20]L. W. Beeferman, Ph. D. thesis, Harvard University, 1970 (unpublished).
[21]D. Pines, *Elementary Excitations in Solids* (Benjamin, New York, 1963), p. 25.
[22]H. Ehrenreich, in *Proceedings of the International School of Physics Enrico Fermi*, edited by J. Tauc (Academic, New York, 1966), Vol. 34, p. 106.
[23]P. C. Martin, in *Many Body Physics* , edited by C. DeWitt and R. Balian (Gordon and Breach, New York, 1968), p. 37.
[24]J. S. Langer, Phys. Rev. 127, 5 (1962).
[25]V. Ambegaokar, in 1962 *Brandeis Summer Institute Lectures* (Benjamin, New York, 1963), Vol. 2, p. 321.
[26]A. J. Layzer, Phys. Rev. 129, 897 (1963).
[27]Because we are dealing with the quasiparticle wave functions, if U_Q represents a pseudopotential, it should contain at least the self-consistent Hartree screening.
[28]That our estimation procedure yields reasonable results is confirmed by a comparison of results using comparable procedures and those obtained by Mahan (Ref. 10) via machine calculations.
[29]P. N. Butcher, Proc. Phys. Soc. (London) 64, 765 (1951).
[30]B. Segall, Phys. Rev. 124, 1797 (1961).
[31]N. W. Ashcroft, Phil. Mag. 8, 2055 (1963).
[32]After completion of this manuscript, recent measurements for Al by Beaglehole came to our attention. Above 1 eV, his curve for the interband contribution to ϵ_2 has a shape very similar to that obtained in Ref. 4 from an analysis of experimental data. However, his values are consistently larger than those of Ref. 4 by almost a factor of 2 in the 1–3-eV range. In addition, he finds some evidence for weak structure near 0.8 eV. G. Dresselhaus and M. S. Dresselhaus, using their Fourier-expansion method, have performed calculations within the RPA based on the Ashcroft band structure which agree well with the Beaglehole data. These therefore provide further confirmation that the interband calculations of ϵ_2 presented in Ref. 4 are too small. We should like to thank the authors involved for making their results available to us before publication.
[33]B. A. Politzer, N. N. Miskovsky, and P. H. Cutler, Phys. Letters 27A, 554 (1968).
[34]P. H. Cutler (private communication).
[35]We are grateful to B. Segall for some discussions of this point.